Nova Scotia Research Foundation Corporation
Dartmouth, Nova Scotia

TECHNOLOGY IN ACTION

THE EFFECT OF DISPERSANT AND STABILIZER TYPE AND AMOUNT ON THE ATOMIZATION OF COAL-WATER FUEL

BY

NEIL STOVER

March, 1989

A PROJECT SPONSORED BY THE DSS 50/50 PROPOSAL PROGRAM, EMR CANADA AND THE CAPE BRETON DEVELOPMENT CORPORATION

DSS Contract No. 23440-7-9183/01-SQ
Scientific Authority: Dr. K. Thambimuthu

NOVA SCOTIA RESEARCH FOUNDATION CORPORATION
P.O. Box 790, Dartmouth, Nova Scotia, Canada, B2Y 3Z7
Tel: (902) 424-8670
Telex: 019-22719
Telecopier: (902) 465-7384

74 pp

MICROMEDIA

TABLE OF CONTENTS

		PAGE
LIST OF FIGURES		ii
LIST OF TABLES		vi
LIST OF PHOTOGRAPHS		vi
NOMENCLATURE		vii
1	ABSTRACT	1
2	INTRODUCTION	2
3	EXPERIMENTAL	2
4	RESULTS AND DISCUSSION	3
5	CONCLUSIONS	33
ACKNOWLEDGEMENTS		36
REFERENCES		36
APPENDIX A - Spray Test Operational Data		

LIST OF FIGURES

		PAGE
Figure 1	Schematic of the NSRFC CWF Atomization Test Facility	39
Figure 2	Schematic of the NRC CWF Atomizer	40
Figure 3	CWF A, Variation of PSD from A,100,100	41
Figure 4	CWF B, Variation of PSD from B,100,100	41
Figure 5	CWF D, variation of PSD from D,100,100	42
Figure 6	Air Post Set A, CWF A, Mixing Chamber GAP 0.61 mm, 3 lbs	43
Figure 7	Air Post Set A, CWF A, Mixing Chamber GAP 0.76 mm, 3 lbs	43
Figure 8	Air Post Set A, CWF A, Mixing Chamber GAP 0.89 mm, 3 lbs	43
Figure 9	Air Post Set A, CWF A, Mixing Chamber GAP 0.61 mm, 5 lbs	44
Figure 10	Air Post Set A, CWF A, Mixing Chamber GAP 0.76 mm, 5 lbs	44
Figure 11	Air Post Set A, CWF A, Mixing Chamber GAP 0.89 mm, 5 lbs	44
Figure 12	Air Post Set B, CWF A, Mixing Chamber GAP 0.61 mm, 3 lbs	45
Figure 13	Air Post Set B, CWF A, Mixing Chamber GAP 0.76 mm, 3 lbs	45
Figure 14	Air Post Set B, CWF A, Mixing Chamber GAP 0.89 mm, 3 lbs	45
Figure 15	Air Post Set B, CWF A, Mixing Chamber GAP 0.61 mm, 5 lbs	46
Figure 16	Air Post Set B, CWF A, Mixing Chamber GAP 0.76 mm, 5 lbs	46
Figure 17	Air Post Set B, CWF A, Mixing Chamber GAP 0.89 mm, 5 lbs	46
Figure 18	Air Post Set D, CWF A, Mixing Chamber GAP 0.61 mm, 3 lbs	47
Figure 19	Air Post Set D, CWF A, Mixing Chamber GAP 0.76 mm, 3 lbs	47
Figure 20	Air Post Set D, CWF A, Mixing Chamber GAP 0.89 mm, 3 lbs	47
Figure 21	Air Post Set D, CWF A, Mixing Chamber GAP 0.61 mm, 5 lbs	48
Figure 22	Air Post Set D, CWF A, Mixing Chamber GAP 0.76 mm, 5 lbs	48
Figure 23	Air Post Set D, CWF A, Mixing Chamber GAP 0.89 mm, 5 lbs	48
Figure 24	A,100,100, Variable Air Flow Rate, d3,2/Do versus A/F at 25°C	49
Figure 25	A,100,100, Variable Air Flow Rate, d3,2/Do versus A/F at 55°C	49
Figure 26	A,100,100, Variable CWF Flow Rate, d3,2/Do versus A/F at 25°C	49
Figure 27	A,100,100, Variable CWF Flow Rate, d3,2/Do versus A/F at 50°C	49
Figure 28	B,100,100, Variable Air Flow Rate, d3,2/Do versus A/F at 25°C	50
Figure 29	B,100,100, Variable Air Flow Rate, d3,2/Do versus A/F at 65°C	50

LIST OF FIGURES (Continued)

		PAGE
Figure 30	B,100,100, Variable CWF Flow Rate, d3,2/Do versus A/F at 25°C	50
Figure 31	B,100,100, Variable CWF Flow Rate, d3,2/Do versus A/F at 55°C	50
Figure 32	C,100,100, Variable Air Flow Rate, d3,2/Do versus A/F at 25°C	51
Figure 33	C,100,100, Variable Air Flow Rate, d3,2/Do versus A/F at 55°C	51
Figure 34	C,100,100, Variable CWF Flow Rate, d3,2/Do versus A/F at 25°C	51
Figure 35	C,100,100, Variable CWF Flow Rate, d3,2/Do versus A/F at 55°C	51
Figure 36	D,100,100, Variable Air Flow Rate, d3,2/Do versus A/F at 25°C	52
Figure 37	D,100,100, Variable Air Flow Rate, d3,2/Do versus A/F at 55°C	52
Figure 38	D,100,100, Variable CWF Flow Rate, d3,2/Do versus A/F at 25°C	52
Figure 39	D,100,100, Variable CWF Flow Rate, d3,2/Do versus A/F at 65°C	52
Figure 40	A,100,100, Average d3,2/Do versus Radial Position	53
Figure 41	B,100,100, Average d3,2/Do versus Radial Position	53
Figure 42	C,100,100, Average d3,2/Do versus Radial Position	53
Figure 43	D,100,100, Average d3,2/Do versus Radial Position	53
Figure 44	Comparison of d3,2/Do versus A/F, CWF A, B, C, D, Variable Air Data	54
Figure 45	Comparison of d3,2/Do versus A/F, CWF A, B, C, D, Variable CWF Data	54
Figure 46	A,100,0, Variable Air Flow Rate, d3,2/Do versus A/F	55
Figure 47	A,100,0, Variable CWF Flow Rate, d3,2/Do versus A/F	55
Figure 48	A,100,50, Variable Air Flow Rate, d3,2/Do versus A/F	55
Figure 49	A,100,50, Variable CWF Flow Rate, d3,2/Do versus A/F	55
Figure 50	A,100,164, Variable Air Flow Rate, d3,2/Do versus A/F	56
Figure 51	A,100,164, Variable CWF Flow Rate, d3,2/Do versus A/F	56
Figure 52	A,240,100, Variable Air Flow Rate, d3,2/Do versus A/F	56
Figure 53	A,240,100, Variable CWF Flow Rate, d3,2/Do versus A/F	56

LIST OF FIGURES (Continued)

		PAGE
Figure 54	A,75,100, Variable Air Flow Rate, d3,2/Do versus A/F	57
Figure 55	A,75,100, Variable CWF Flow Rate, d3,2/Do versus A/F	57
Figure 56	A,100,0, Radial Position Data, d3,2/Do versus A/F	57
Figure 57	A,100,50, Radial Position Data, d3,2/Do versus A/F	57
Figure 58	A,100,164, Radial Position Data, d3,2/Do versus A/F	58
Figure 59	A,240,100, Radial Position Data, d3,2/Do versus A/F	58
Figure 60	A,75,100, Radial Position Data, d3,2/Do versus A/F	58
Figure 61	Difference of d3,2/Do versus A/F for Variable Air Flow, as CWF A Stabilizer Amount is Varied	59
Figure 62	Difference of d3,2/Do versus A/F for Variable Air Flow, as CWF A Dispersant Amount is Varied	59
Figure 63	Difference of d3,2/Do versus A/F for Variable CWF Flow, as CWF A Dispersant Amount is Varied	59
Figure 64	Difference of d3,2/Do versus A/F for Variable CWF Flow, as CWF A Stabilizer Amount is Varied	59
Figure 65	B,100,0, Variable Air Flow Rate, d3,2/Do versus A/F	60
Figure 66	B,100,0, Variable CWF Flow Rate, d3,2/Do versus A/F	60
Figure 67	B,100,260, Variable Air Flow Rate, d3,2/Do versus A/F	60
Figure 68	B,100,260, Variable CWF Flow Rate, d3,2/Do versus A/F	60
Figure 69	B,200,100, Variable Air Flow Rate, d3,2/Do versus A/F	61
Figure 70	B,200,100, Variable CWF Flow Rate, d3,2/Do versus A/F	61
Figure 71	B,75,100, Variable Air Flow Rate, d3,2/Do versus A/F	61
Figure 72	B,75,100, Variable CWF Flow Rate, d3,2/Do versus A/F	61
Figure 73	B,100,0, Radial Position Data, d3,2/Do versus A/F	62
Figure 74	B,100,260, Radial Position Data, d3,2/Do versus A/F	62
Figure 75	B,200,100, Radial Position Data, d3,2/Do versus A/F	62
Figure 76	B,75,100, Radial Position Data, d3,2/Do versus A/F	62
Figure 77	Difference of d3,2/Do versus A/F for Variable Air Flow, as CWF B Dispersant Amount is Varied	63
Figure 78	Difference of d3,2/Do versus A/F for Variable Air Flow, as CWF B Stabilizer Amount is Varied	63

LIST OF FIGURES (Continued)

		PAGE
Figure 79	Difference of d3,2/Do versus A/F for Variable CWF Flow, as CWF B Dispersant Amount is Varied	63
Figure 80	Difference of d3,2/Do versus A/F for Variable CWF Flow, as CWF B Stabilizer Amount is Varied	63
Figure 81	D,100,150, Variable Air Flow Rate, d3,2/Do versus A/F	64
Figure 82	D,100,150, Variable CWF Flow Rate, d3,2/Do versus A/F	64
Figure 83	D,100,50, Variable Air Flow Rate, d3,2/Do versus A/F	64
Figure 84	D,100,50, Variable CWF Flow Rate, d3,2/Do versus A/F	64
Figure 85	D,100,150, Radial Position Data, d3,2/Do versus A/F	65
Figure 86	D,100,50, Radial Position Data, d3,2/Do versus A/F	65
Figure 87	Difference of d3,2/Do versus A/F for Variable Air Flow, as CWF D Stabilizer Amount is Varied	65
Figure 88	Difference of d3,2/Do versus A/F for Variable CWF Flow, as CWF D Stabilizer Amount is Varied	65
Figure 89	Instrumental Atomizer, Mixing Chamber Pressure Versus Air Mass Flow Rate	66
Figure 90	Instrumental Atomizer, Mixing Chamber Pressure Versus Liquid Mass Flow Rate	66

LIST OF TABLES

		PAGE
Table 1	The CWF Configurations Tested	3
Table 2	CWF Analysis Provided by CBDC	5
Table 3	Low Shear Rate Rheology Data	6
Table 4	Reduction in Apparent Viscosity with a 1% Increase in Water Content	8
Table 5	Dynamic Yield Stress Data	10
Table 6	High Shear Rate Rheology Data	12
Table 7	Surface Tension Data	14
Table 8	Atomization Correlations	21

LIST OF PHOTOGRAPHS

		PAGE
PHOTO 1	CWF A100,100, 3.2E-2 kg/s, ALR = 0.19	37
PHOTO 2	CWF B100,240, 3.2E-2 kg/s, ALR = 0.19	37
PHOTO 3	Instrumented NRCC Atomizer	38

NOMEMCLATURE

Symbol	Description	Units
A	CWF configuration d1,s1	/
A1	Atomizer mixing chamber exit area	m^2
ALR	Air to fuel mass flow ratio	/
B	CWF configuration d2,s1	/
C	CWF configuration d3,s1	/
Cd	Drag coefficient of a spray droplet	/
D	CWF configuration d1,s2	/
d	Equilibrium drop diameter	μm
d1	Dispersant chemical number 1 destination	/
d2	Dispersant chemical number 2 destination	/
d3	Dispersant chemical number 3 destination	/
d3,2	Sauter mean diameter	μm
da1	Atomizer air channel diameter	m
da2	Atomizer air post diameter	m
dc	Atomizer cone large diameter	m
de	4 * wetted area/ wetted perimeter	m
Do	Characteristic exit diameter of atomizer	m
dr	Atomizer ring exit diameter	m
G	Atomizer mixing chamber gap width	m
L	Atomizer mixing chamber length	m
ma	Molecular weight of air	kg/(kg*mole)
mvg	Molar volume of a gas	m^3/(kg*mole)
n	Flow index	/
Pa	Atomizing air pressure at the measuring device	Pa
Qa	Mass flow rate of air	kg/s
s1	Stabilizer chemical number 1 destination	/
s2	Stabilizer chemical number 2 destination	/
Ta	Atomizing air temperature	°C
Va	Air velocity at atomizer exit	m/s
τ	Shear stress	mPa
γ	Shear rate	s^{-1}
μa	Apparent viscosity	mPa*s
τ'	Yield stress	mPa
ρ	Atomizing air density	kg/m^3
σ	CWF surface tension	N/m^2

1. ABSTRACT

The effect of varying the dispersant and stabilizer type and amount on the atomization of coal-water fuel (CWF) has been investigated.

Atomization of the CWF's was carried out using an air-blast prefilming internal mix atomizer. The atomized CWF particle size distribution has been represented in the form of a surface area mean diameter or d3,2.

The effect of the concentration of the dispersant on the surface tension of the CWF and filtrates varied as the stabilizer that the dispersant was combined with was changed. The effect of the stabilizer concentration on surface tension was also dependant upon the chemical that it was combined with.

Variations in the CWF water content, that were within the production limits, masked the effect of varying the chemical type and amount on the low shear rate rheology of the CWF's in some cases. Increasing either the dispersant or stabilizer concentration caused an increase in the low shear rate viscosity of the CWF's.

Significant variations were seen PSD of the coal in the CWF's. The effect of the coal PSD on the CWF atomization has not been quantified in this work.

Comparison of the atomization data for the CWF configurations with the standard concentration of both dispersant and stabilizer showed the CWF D configuration to atomize the worst. Anomalies in the atomization and characterization data for the various CWF D configurations could not be explained.

Increasing either the dispersant or stabilizer concentrations resulted in an increased d3,2 value. The increase in the d3,2 as compared to the normal concentration CWF decreased as the ALR was increased.

2. INTRODUCTION

The Cape Breton Development Corporation (CBDC) has chosen to market some of it's coal in the form of coal-water fuel (CWF). The proper formulation of the CWF requires the addition of a dispersant to allow the hydrophobic coal surface to be wetted and a stabilizer that prevents the settling of the coal. Besides effecting the economics of the CWF production these chemicals effect the CWF atomization properties.

The Nova Scotia Research Foundation Corporation (NSRFC) has undertaken a project to examine the effect of the dispersant and stabilizer type and amount has on the CWF atomization.

A single CWF atomizer design has been used to atomize the CWF with a constant coal feed stock and coal particle size distribution.

3. EXPERIMENTAL

A schematic of the NSRFC CWF Atomization Test Facility is shown in Figure 1.

The CWF was pumped into a 700 litre day tank prior to the atomization tests. From the day tank, a positive displacement progressing cavity pump transferred the CWF to the spray chamber.

The atomizer sprays vertically downward in the 1 by 1.5 m CWF spray chamber. The atomizer is rotated to ensure that a representative spray droplet size measurement is made. A Malvern Model 3600 is used to size the CWF spray droplets.

Compressed air is supplied to the atomizer from a 22 kw rotary screw compressor. The air mass flow rate is determined from the volumetric flow, temperature and pressure.

A Haake Model RV 11 rotational viscometer is used to examine the low shear rate rheology of the CWF. An extrusion type rheometer is used to obtain shear rates similar to those encountered in the atomizer (ie 10,000 s^{-1}).

Surface tensions of the CWF's and their filtrates were measured using a Fisher Tenseomat Model 21 ring type device and a drop weight type apparatus constructed at NSRFC.

An atomizer designed by the National Research Council of Canada (NRC) was used during all of the atomization tests.

4. RESULTS AND DISCUSSION

4-1 LABORATORY DATA

This section contains all of the data pertaining to the CWF's tested in this project.

4-1-1 List of CWF Configurations

Table 1 lists the various CWF configurations that were tested.

A,100,0	B,100,0
A,100,100	B,100,100
A,100,169	B,100,260
A,100,50	B,200,100
A,240,100	B,75,100
A,75,100	
C,100,100	D,100,100
	D,100,150
	D,100,50

Table 1, The CWF Configurations Tested

In Table 1, the letter preceding the numbers indicates the combination of dispersant and stabilizer used in the CWF configuration. The dispersants are added to allow the hydrophobic coal surface to be wetted by reducing the interfacial surface tension between the coal and the water and thus permitting the formation of a low water content CWF. The stabilizer prevents the coal in the CWF from settling out when at rest during storage. Specific information regarding the nature of the chemical additives is proprietary and will not be discussed in this report. The numbers following the additive denotation letter indicate the percentage of the "normal" concentration of the stabilizer and dispersant respectively. Four combinations of dispersants and stabilizers were tested and called A, B, C and D.

The dispersant in CWF's A and D was the same chemical while CWF's C and B had a second and third type of dispersant. CWF's A, B and C had the same stabilizer. The various configurations can be represented as follows;

$$A = d1,s1 \quad B = d2,s1 \quad C = d3,s1 \quad D = d1,s2$$

The rational for varying the additive type and amount as shown above is as follows. The limitation on the dispersant concentration is set by the allowable low shear rate viscosity and the amount needed to insure the efficient wetting of the coal surface. The limitation on the stabilizer concentration is from none, an unstable short storage time CWF, to what is considered to be the acceptable upper viscosity range.

CWF A is considered to be the "Base Case" configuration and subsequently had both the dispersant and stabilizer varied to determine the effect on atomization. In so much as CWF D had the same dispersant as CWF A, the dispersant concentration was not varied in CWF D. The stabilizer in CWF D was different from that used in CWF A and was therefore varied.

The use of the d2 dispersant in CWF B only, necessitated the variation of its concentration. Despite the fact that CWF B had the same stabilizer as CWF A (s1), it was deemed appropriate to vary the stabilizer concentration to determine if the combinations of dispersant and stabilizer effected the atomization in different manors.

CWF C proved troublesome to handle and only the regular concentrations of dispersant and stabilizer were tested.

4-1-2 Ash, Density and Moisture

Table 2 shows a summary of the CWF's tested in this project. The data in Table 2 has been provided by the CWF manufacturer, the Cape Breton Development Corporation. Table 2 shows the CWF ash percentage, density and the water content.

	CWF	ASH (%)	DENSITY (kg/m^3)	MOISTURE (%)
	A,100,0	2.79	1100	28.50
*1	A,100,100	4.33	1200	29.93
*2	A,100,100	4.30	1190	31.30
*3	A,100,100	4.30	1200	28.93
	A,100,169	3.39	1190	30.93
	A,100,50	1.90	1165	31.83
	A,240,100	4.10	1200	31.30
	A,75,100	2.56	1162	30.24
	B,100,0	2.37	1178	30.00
	B,100,100	4.10	1220	30.60
	B,100,260	4.14	1200	32.20
	B,200,100	4.40	1180	31.82
	B,75,100	5.13	1210	29.95
	C,100,100	2.21	1030	33.00
	D,100,100	2.49	1190	31.08
	D,100,150	2.82	1120	29.25
	D,100,50	2.76	1088	30.18

* - denotes different batches of the same CWF configuration.

Table 2, CWF Analysis Provided by CBDC

The ash contents ranged from 1.90 to 5.13 percent and reflect the degree of cleaning and the parent coal composition. The majority of the densities were approximately 1200 kg/m^3. The moisture percentage variation was small but is significant in relation to the low shear rate rheological properties. In particular, the moisture content of the various batches of CWF A,100,100 varied by 3.63 percent.

4-1-3 Low Shear Rate Rheology

The primary reason for carrying out the low shear rate rheology tests was to have a standard characterization of the CWF. Direct correlations between the low shear rate rheology and the atomization performance of a CWF have not been clearly established. The low shear rate data does allow a determination of the stability and handling characteristics of the CWF. In addition, any variation from batch to batch can be identified and investigated.

Other factors may effect the low shear rate rheology. Variations in the coal particle size distribution will have an effect which is difficult to quantify. Table 3 shows the low shear rate rheological properties of the CWF's atomized in this study.

CWF (batch #)	TEMP.	% H_2O	THIXOTROPY ******* cycle *******			APPARENT VISCOSITY AT 100 s^{-1} 3 rd CYCLE RETURN
			1 st	2 nd	3 rd	
	(°C)		(J)	(J)	(J)	(mPa.s)
A,100,100,1	25	31.30	25.9	4.5	3.2	720
A,100,100,1	65	31.30	31.3	5.7	1.6	260
A,100,100,2	25	29.93	34.4	5.3	2.3	720
A,100,100,2	25	30.93 *	26.1	5.5	1.8	640
A,100,100,2	65	29.93	27.4	4.9	1.5	360
A,100,100,2	65	30.93 *	24.0	3.4	0.9	300
A,100,0	25	28.50	32.8	5.2	1.7	360
A,240,100	25	31.30	27.0	8.9	4.8	1040
A,100,164	25	30.93	22.4	7.6	4.0	1000
A,75,100	25	30.24	23.0	4.2	1.5	570
A,75,100	65	30.24	26.5	17.9	17.9	800
A,100,50	25	31.83	6.7	1.3	0.6	125
A,100,50	65	31.83	8.8	0.4	1.8	128

* indicates the water content of the CWF was increased at NSRFC by 1 %

Table 3, Low Shear Rate Rheology Data

CWF (batch #)	TEMP. (°C)	% H_2O	THIXOTROPY ******* cycle ******* 1 st (J)	2 nd (J)	3 rd (J)	APPARENT VISCOSITY AT 100 s^{-1} 3 rd CYCLE RETURN (mPa.s)
B,100,100	25	30.60	29.5	7.0	1.5	680
B,100,100	65	30.60	40.4	19.9	18.4	560
B,100,260	25	32.20	18.8	6.8	3.9	1250
B,100,260	65	32.20	35.3	-11.9	-8.6	1100
B,200,100	25	31.82	28.8	5.9	2.3	1150
B,200,100	65	31.82	11.0	6.5	29.4	500
B,75,100	25	29.95	38.8	8.5	3.4	850
B,75,100	65	29.95	36.3	-10.2	-13.2	850
B,100,0	25	30.00	21.5	1.7	0.7	200
B,100,0	65	30.00	22.2	5.3	3.6	160

CWF (batch #)	TEMP. (°C)	% H_2O	THIXOTROPY ******* cycle ******* 1 st (J)	2 nd (J)	3 rd (J)	APPARENT VISCOSITY AT 100 s^{-1} 3 rd CYCLE RETURN (mPa.s)
C,100,100	25	33.00	24.3	-5.2	-7.6	1500
C,100,100	25	34.00 *	31.9	4.0	1.1	1000
D,100,100	25	30.08	54.3	6.8	-5.1	1000
D,100,100	25	31.08 *	22.4	-2.0	-4.1	840
D,100,100	65	30.08	7.1	26.9	24.0	800
D,100,100	65	31.08 *	26.4	24.7	15.9	790
D,100,50	25	30.18	9.0	3.3	1.5	540
D,100,50	65	30.18	1.4	0.4	1.7	300
D,100,150	25	29.25	43.8	13.4	5.4	820
D,100,150	65	29.25	55.9	14.0	4.4	190

* indicates the water content of the CWF was increased by 1 % at NSRFC.

Table 3, Low Shear Rate Rheology Data, continued.

The data in Table 3 were generated following the procedures of Worchal, et al (1).* Each CWF was subject to three cycles of increasing shear rate to 150 s^{-1} taking six minutes, constant shear rate at 150 s^{-1} for two minutes and decreasing shear rate for six minutes to 0 s^{-1}.

The apparent viscosity is equal to the slope of the shear stress versus shear rate curve;

$$\mu a = \tau/\gamma \qquad (4.1)$$

The degree of thixotropy, which is the area inside a shear stress versus shear rate cycle, is reported for each cycle. A positive thixotropy indicates that the shear stress decreased with time (i.e. the shear stress was less, at the same shear rate, during the decreasing shear rate portion of the cycle than the increasing shear rate portion of the cycle). The apparent viscosity is reported from the value obtained at a shear rate of 100 s^{-1} on the decreasing shear rate portion of the third cycle.

In some cases the tests were repeated at a raised temperature to evaluate the temperature sensitivity of the CWF rheology. The water content of some of the CWF's was varied at NSRFC to examine the effect on the rheology.

Care must be exercised when examining the effect of temperature and additive type and amount on the low shear rate rheology due to what might be over powering effects of the normal variations in the water content of the CWF as it is produced (see Table 2). Table 4 shows the reduction in the apparent viscosity at 25°C when the water content was increased by 1 percent;

CWF	Temperature (°C)	Viscosity Reduction (mPa.s)
A,100,100	25	80
A,100,100	65	60
C,100,100	25	500
D,100,100	25	160
D,100,100	65	10

Table 4, Reduction in Apparent Viscosity With a 1 % Increase in Water Content

* Numbers in brackets indicate references.

The apparent viscosity of a CWF will decrease as the dispersant concentration is increased from zero as the wetting of the coal surface in enhanced. A point is reached where the interfacial surface tension is reduced such that the increased attraction of the water to the coal surface begins to result in an increased viscosity. CWF's are typically made with the dispersant concentration such that the viscosity is at its minimum value. The CWF's tested here have their normal concentration denoted as the 100 percent.

For CWF A, it can be seen in Table 3 that as the dispersant concentration is raised from 75 to 240%, while the stabilizer concentration is held constant, that the viscosity increases despite a 0.9% increase in the CWF water content. The addition of stabilizer increases the viscosity continuously as it's concentration is increased.

Similar trends are seen for CWF B except for the case of B,75,100. Here a decrease in the viscosity would be expected from the B,100,100 case but an increase is seen. This may be explained by the decrease in the water content of B,75,100 in relation to B,100,100.

It would be expected that as the stabilizer concentration is increased that the low shear rate viscosity would increase continuously with all other factors held constant. For CWF A the viscosity decreases as the stabilizer concentration is increased from 0 to 50%. This would be explained by the 3.5% increase in the water content.

The viscosity of CWF B increases continuously as the stabilizer concentration is increased.

For CWF D, when the stabilizer concentration was decreased (D,100,50) the viscosity dropped. A decrease was also seen for the D,100,150, despite the decrease in the water content. This result cannot be explained from the data available.

4-1-4 Yield Stress

During the atomization of CWF, the forces which resist the deformation and subsequent disintegration of larger CWF drops to smaller ones include the viscous resistance. An attempt has been made to quantify the dynamic yield stress of the CWF which may play a role during the CWF drop formation process. Table 5 shows the dynamic yield stress data for the CWF's atomized.

CWF A Variable Stabilizer s1	DYNAMIC YIELD STRESS (mPa)	CWF B Variable Stabilize s1	DYNAMIC YIELD STRESS (mPa)
0	0.33	0	0.27
50	3.35	100	2.96
100	2.78	260	10.5
100	3.03		
164	4.35		

CWF D Variable Stabilizer s2	DYNAMIC YIELD STRESS (mPa)
50	1.43
100	3.04
150	2.24

CWF A Variable Dispersant d1	DYNAMIC YIELD STRESS (mPa)	CWF B Variable Dispersant d2	DYNAMIC YIELD STRESS (mPa)
75	1.19	75	3
100	2.78	100	2.96
240	2.52	200	8.6

Table 5, Dynamic Yield Stress Data

The stabilizers used in the CWF's are long chain polymers that are dispersed in the liquid phase. When the CWF is not being sheared (pumped), the stabilizers retard the movement of the coal particles under the force of gravity thereby preventing settling. Ideally, as the CWF is sheared, the resistance to the coal particles moving past each other will diminish and the pumping energy needs will be reduced. This characteristic is evidenced in the pseudoplastic (shear stress reduces with shear rate) behaviour of the CWF. An extension of this characteristic is that a certain shear stress must be applied prior to the initial deformation of the CWF. This initial shear stress is called the yield stress. Equation 1 is modified as follows to accommodate this yield stress plus pseudoplastic behaviour;

$$\tau = \tau' + \mu a \times \gamma \qquad (4.2)$$

Generally as the stabilizer or dispersant amount is increased the yield stress increases. Variations in these trends cannot be explained from the data obtained in this report. As the concentration of dispersant d1 is increased in CWF A the yield stress increases and then levels off. Increasing the concentration of dispersant d2 in CWF B results in a much more dramatic increase in the yield stress. This data may be interpreted as indicating the degree to which the dispersant attracts the water to the coal surface. A similar trend was seen in the low shear rate rheology data for CWF's A and B. An increase in stabilizer s2 in CWF D did not result in the same increase in the yield stress as seen in CWF A.

4-1-5 High Shear Rate Rheology

The CWF's were subject to high shear rheology tests in order to determine if these characteristics would show any trends that might be correlatable to the atomization results.

The model, as described in the Experimental section, was used to generate the rheological data in the form;

$$\tau = k \times \gamma^n \qquad (4.3)$$

Where n is the flow index. If $n < 1$ then the CWF is pseudoplastic, $n = 1$ then Newtonian and if $n > 1$ then the CWF is dilatant according to the model. For all of the tests, μa either increased or decreased rapidly at the lower shear rates and then asymptoticly approached the equilibrium apparent viscosities shown in Table 6.

CWF	TEMP °C	MAX SHEAR RATE (s^{-1})	k	n	EQUILIBRIUM APPARENT VISCOSITY
A,100,0	21	5100	1.06E+01	0.85	625
A,100,50	22	5500	3.76E-01	1.02	440
A,100,100	23	11500	2.46E-01	0.95	160
A,100,100	65	18000	3.53E-03	1.38	155
A,100,164	22	7700	1.79E+00	0.83	390
A,75,100	22	4500	6.90E+00	0.68	460
A,240,100	22	9000	1.06E+01	0.54	155
B,100,0	27	8000	1.11E-01	1.10	280
B,100,100	55	13500	1.65E+00	0.77	175
B,100,100	18	5500	3.80E+00	0.75	445
B,100,260	21	6000	7.08E-01	0.94	430
B,75,100	26	4500	1.88E+01	0.85	525
B,200,100	21	5000	5.14E+00	0.72	460
C,100,100	20	7500	1.91E-01	1.11	510
D,100,50	25	5700	2.61E-01	1.07	495
D,100,100	22	3800	4.85E-02	1.34	820
D,100,100	65	1200	7.49E-01	0.85	185
D,100,150	22	5000	2.55E-01	1.13	780

Table 6, High Shear Rate Rheology Data

As the temperature of CWF A,100,100 was raised μa did not change appreciably. For CWF's B and D, μa decreased markedly as the temperature was raised.

The highly pseudoplastic or dilatant behaviour of the CWF's as indicated by the power index, n, must be examined with some care. All of the CWF's exhibited a characteristic rapid rise or fall followed by an asymptotic approach to the equilibrium viscosity. This leaves the interpretation of the strongly pseudoplastic or dilatant characteristics of the CWF's in question.

For CWF's A and B, as the concentrations of dispersants d1 and d2 were increased, the equilibrium viscosity decreased and then remained constant. Despite the fact that the equilibrium viscosity is in the same order of magnitude as the low shear rate data, the trends with the dispersant concentration is opposite.

As the stabilizer concentration in CWF A is increased the equilibrium viscosity decreases up to the 100% concentration and then increases. The initial decrease can be attributed to the increase in the water content (28.5 to 31.8%). The further decrease cannot be attributed to the water content, as it actually decreases slightly from 31.8 to 31.3 percent. It is possible that the coal particle size distribution may be effecting the high shear rate viscosity.

For CWF B, as the stabilizer concentration was increased, the equilibrium viscosity increased despite the variation in the water content.

As the dispersant concentration in CWF D was increased, the equilibrium viscosity increased and then decreased. The decrease from the 100 to 150 percent stabilizer concentration cannot be accounted for especially when considering that the water concentration decreased from 31.1 to 29.3 percent as the dispersant concentration was increased.

4-1-6 CWF and CWF Filtrate Surface Tensions

The effect of the dispersant type and concentration on the CWF atomization will be dependant upon the mechanisms that are controlling the atomization process. For single phase atomization, the surface tension of the liquid has opposing effects depending upon the stage of the drop formation process (2). Deformation of the liquid sheet, which causes an increase in the surface area, is resisted by the surface tension force which attempts to minimize the surface to volume ratio. If the forces which are causing the deformation (mechanical and aerodynamic) overcome the resistance of the surface tension, the deformation will increase in size to form a ligament and the surface tension assists the disintegration by forming a sphere (3).

During the atomization of CWF the strongest forces resisting the deformation of the bulk CWF will be those associated with the rheology. The formation of the smaller drops may be effected by the surface tension forces in the CWF. The point of cleavage of the CWF into smaller drops may be in the liquid phase, in which case the surface tension of importance would be that of the liquid. The surface tension of a liquid surface takes some time to develop. The time of drop formation is much less than the surface tension development time, therefore only the surface tension the pure liquid (water) is relevant (4,5). If the cleavage of the larger drop into smaller drops takes place at the coal/liquid interface, then the interfacial surface tension of the coal/liquid will be of relevance during the CWF atomization. Measurement of the coal/liquid interfacial surface tension can be made using a contact angle method. This method requires the preparation of the coal surface thereby alternating it from the condition that it would be in a CWF. An attempt has been made to estimate the CWF and CWF filtrate surface tension using both a ring and drop weight type apparatus (Table 7).

LIQUID		METHOD (R or D)	SURF.TEN (kg/m)	STD.DEV.
A100,100	CWF	D	0.082	2.6E-03
A100,100	FILTRATE	D	0.055	4.3E-04
A100,100	CWF	R	0.061	4.1E-04
A100,100	FILTRATE	R	0.060	1.5E-04
A100,0	CWF	D	0.061	1.4E-03
A100,0	FILTRATE	D	0.057	3.5E-04
A100,0	CWF	R	0.057	1.2E-04
A100,0	FILTRATE	R	0.050	6.3E-04
A240,100	CWF	D	0.056	3.7E-03
A240,100	FILTRATE	D	0.048	1.7E-03
A240,100	CWF	R	0.060	3.6E-04
A240,100	FILTRATE	R	0.050	9.4E-05
A100,164	CWF	D	0.070	6.7E-03
A100,164	FILTRATE	D	0.058	2.3E-03
A100,164	CWF	R	0.065	3.6E-04
A100,164	FILTRATE	R	0.054	3.4E-04
A100,50	CWF	D	0.067	5.9E-04
A100,50	FILTRATE	D	0.056	2.2E-04
A100,50	CWF	R	0.053	7.1E-05
A100,50	FILTRATE	R	0.054	4.4E-04
A75,100	CWF	D	0.054	5.4E-04
A75,100	FILTRATE	D	0.061	3.0E-04
A75,100	CWF	R	0.063	8.2E-05
A75,100	FILTRATE	R	0.059	2.9E-04

Table 7, Surface Tension Data

LIQUID		METHOD (R or D)	SURF.TEN (kg/m)	STD.DEV.
B100,100	CWF	D	0.043	7.9E-04
B100,100	FILTRATE	D	0.045	1.1E-03
B100,100	CWF	R	0.062	4.3E-04
B100,100	FILTRATE	R	0.058	3.1E-04
B100,260	CWF	D	0.068	1.7E-03
B100,260	FILTRATE	D	0.054	8.2E-04
B100,260	CWF	R	0.071	5.3E-04
B100,260	FILTRATE	R	0.055	4.3E-04
B100,0	CWF	D	0.046	1.2E-03
B100,0	FILTRATE	D	0.062	3.5E-03
B100,0	CWF	R	0.058	8.2E-05
B100,0	FILTRATE	R	0.058	8.2E-05
B75,100	CWF	D	0.046	2.1E-03
B75,100	FILTRATE	D	0.061	3.6E-03
B75,100	CWF	R	0.069	8.3E-04
B75,100	FILTRATE	R	0.060	1.2E-04
B200,100	CWF	D	0.053	5.3E-04
B200,100	FILTRATE	D	0.062	4.0E-03
B200,100	CWF	R	0.069	2.2E-04
B200,100	FILTRATE	R	0.057	7.3E-04

Table 7, Surface Tension Data, Continued

LIQUID		METHOD (R or D)	SURF.TEN (kg/m)	STD.DEV.
C100,100	CWF	D	0.089	5.7E-04
C100,100	FILTRATE	D	0.062	2.2E-04
C100,100	CWF	R	0.085	5.1E-04
C100,100	FILTRATE	R	0.059	2.2E-04
D100,100	CWF	D	0.064	2.9E-04
D100,100	FILTRATE	D	0.055	4.4E-04
D100,100	CWF	R	0.065	3.3E-04
D100,100	FILTRATE	R	0.055	5.1E-04
D100,50	CWF	D	0.071	3.5E-03
D100,50	FILTRATE	D	0.062	9.1E-05
D100,50	CWF	R	0.063	2.2E-04
D100,50	FILTRATE	R	0.059	1.2E-04
D100,150	CWF	D	0.060	3.0E-04
D100,150	FILTRATE	D	0.061	8.5E-05
D100,150	CWF	R	0.063	1.1E-04
D100,150	FILTRATE	R	0.055	2.7E-04

Table 7, Surface Tension Data, Concluded

Prior to discussing the surface tension data it is appropriate to reiterate the dispersant and stabilizer configurations as follows;

$$A = d1,s1 \quad B = d2,s1 \quad C = d3,s1 \quad D = d1,s2$$

where the lower cases letters refer to the dispersant and stabilizer type.

As discussed above, the point of cleavage of the CWF drop during atomization determines the surface tension which is relevant (the liquid phase or the liquid/solid interface).

Effect of Additives on the Surface Tension of the Filtrate of the CWF's

The liquid phase surface tension is easily measured using either the ring or drop methods. For CWF filtrate A, the surface tension decreases as the dispersant concentration is increased (constant stabilizer amount). The presence of the dispersant in the water would be expected to reduce the surface tension as it interferes with the strong poler attraction of

the water molecules which results in the high surface tension. Neither of the measurement techniques would be affected by the presence of the dispersant. The variation of dispersant d2, in CWF B results in similar trends for the filtrate.

For CWF's A, B and D increasing the stabilizer amount (at constant dispersant amount) resulted in a decrease in the surface tension of the filtrates as measured by the drop method. The slow drop formation rate negates any effect that the very high molecular weight stabilizer may have on the development of the equilibrium between the surface tension and the force of gravity. The ring method showed an increase in the surface tension of CWF A filtrate as the stabilizer amount was increased while CWF's B and D had a decrease. This result cannot be explained considering that CWF's A and B had the same stabilizer chemical.

Effect of Additives on the Surface Tension of the CWF's

The data obtained from the ring method while testing the CWF surface tension must be carefully interpreted. When the ring pulls up from the CWF a meniscus is formed between the ring and the main body of the CWF sample. The meniscus is relatively clearer than the CWF indicating a lower coal content than the CWF. This situation should result in data that more closely resembles the filtrate surface tension.

The drop weight method must have a lengthy drop formation time. This may allow the water to dry from the CWF drop surface. The dried CWF drop surface may then effect the equilibrium drop size and effect the surface tension measurement. If the surface tension data is reliable, then it would be useful in examining the effect of surface tension on equilibrium drop size produced during atomization. As the surface tension increases, the aerodynamic force needed to deform the drop to the point of disintegration increases. The smaller the drop size the greater the aerodynamic force needed to disintegrate it (6). If the cleavage point for the larger drops is at the coal/liquid interface then the coal/liquid interfacial surface tension would play a role during the formation of the drops initially. The aerodynamic drag forces can no longer disintegrate the larger drops into smaller ones when the surface tension of the bulk CWF is capable of resisting.

Table 7 shows that for CWF A, the drop method gives higher values than the ring method but in both cases the surface tension increases as the stabilizer concentration is increased (at a constant dispersant concentration). When the dispersant concentration is increased, no trend can be seen. Similar trends are seen for CWF B as both the stabilizer and dispersant concentrations are increased. CWF D shows the reverse trend to the other CWF's as the stabilizer concentration is increased. This may be attributed to the s2 stabilizer used in CWF D as apposed to the s1 stabilizer in CWF's A and B.

4-1-7 Coal Particle Size Distribution

The coal particle size distribution (PSD) is proprietary information and cannot be discussed in detail in this report. A cryptic version of the PSD data will be presented. When the coal for the CWF is ground controlling the PSD is very important. The coal PSD effects the packing efficiency (7) and the rheological properties of the CWF. The CBDC has an "ideal" coal PSD for their product. For this analysis six particle size distribution groups have been assigned to the PSD data, A, B, C, D, E and F. Where F represents the group with the larger particle measurement size ranges. CBDC has provided NSRFC with the percentage deviation of each size group from the "ideal" for each of the CWF's tested. For each of the CWF's A, B and D, Figures 5, 6 and 7 respectively, show the deviation of the various CWF configurations from their appropriate base case (i.e. CWF A,100,0 is compared to A,100,100,etc.).

An attempt will be made during the discussion of the atomization data to relate the coal PSD data.

4-2 HANDLING RESULTS

4-2-1 Settling in Barrels

In all cases the CWF's were shipped to NSRFC in 300 litre barrels. For the cases of the lower stabilizer concentration CWF's, the CWF's were shipped without delay and their condition checked immediately upon arrival at NSRFC. Where any settling had occurred, the contents of the barrels were resuspended in the barrels as completely as possible and then stirred in the day tank to further homogenize the CWF.

4-2-2 Pressure Variations During Pumping

The operational data tables included in the appendix show the CWF delivery pressure for each test. Some variation in the CWF delivery pressure is seen at a constant CWF flow rate for some of the CWF's. This variation is exclusive of the normally expected increase in the delivery pressure as the atomizing air flow rate, and pressure, is increased. These variations can be attributed to inconsistencies in the CWF as it is pumped through the pipes and screen. The inconsistencies are variations in the water content and flocks of coal particles. The resultant CWF variation, and more importantly, the subsequent variation in the air pressure, would momentarily cause a change in the CWF atomization.

4-2-3 Presence of Oversize Coal Particles and Their Effects

During the CWF production, a certain amount of particles that have diameters greater than desirable remain in the CWF. During the atomization testing at NSRFC, a number of the CWF's had quantities of particles that were larger than the passage ways in the atomizer. The smallest passage way is the one that leads into the mixing chamber from the CWF channel. The presence of an oversize particle serves as a nucleation site for smaller particles to collect on. The rate at which the CWF delivery pressure increases depends upon the relative amount of oversize particles and the CWF flow rate.

4-3 ATOMIZATION TEST RESULTS

In this section the atomization data will be examined and explained. The calculations used to quantify the operational parameters are described below. The correlations using the calculated variables are contained in Table 8.

4-3-1 Photographs of Sprays and Discussion of the NRC atomizer in General

Photographs 1 and 2 show the tip of the NRCC atomizer as the CWF is emanating from it at a flow rate of 3.2E-2 kg/s and ALR of 0.19. Photo 1 shows CWF A100,100 and Photo 2 CWF B100,240.

For CWF A100,100, the atomization appears to be virtually complete as the CWF leaves the mixing chamber. A small amount of CWF in the form of ligaments can be seen in the spray.

The atomization of CWF B100,240 is obviously much worse than that seen for CWF A100,100 in Photo 1. A significant portion of the spray is in the form of large ligaments of CWF which are deforming as they move away from the atomizer tip.

The atomizer exit velocity is calculated as follows;

$$Va = \frac{Qa \times mvg}{ma \times Al} \qquad (4.4)$$

$$\text{where } Al = \frac{(dr^2-(dr-2xG)^2) \times \pi}{4} \qquad (4.5)$$

$$\text{and } Qa = \frac{Va \times 273 \times (Pa+101) \times ma}{(273+Ta) \times Pa \times mvg} \qquad (4.6)$$

The maximum value of Va is 343 m/s or sonic velocity. The density of tair is assumed to be at ambient conditions until Va = Vsonic (343 m/s), then;

$$Va = \frac{Qa}{Vsonic \times Al} \qquad (4.7)$$

For all of the spray droplet size test data, multiple linear regression analysis was carried out to develop equations to fit the experimental data. Table 8 shows all of the atomization data correlations.

CWF	AIR VELOCITY	VARY	TEMP deg C	CONSTANT	1+1/ALR POWER	We POWER
A,100,100	subsonic	AIR	19	1.76E+02	0.000	-0.161
A,100,100	sonic	AIR	19	3.33E+02	0.000	-0.238
A,100,100	subsonic	AIR	55	1.67E+02	0.000	-0.16
A,100,100	sonic	AIR	55	1.52E+03	0.000	-0.443
A,100,100	subsonic	CWF	18	6.24E+01	-0.082	0
A,100,100	sonic	CWF	18	6.70E+01	-0.371	0
A,100,100	subsonic	CWF	55	1.06E+02	-0.494	0
A,100,100	sonic	CWF	55	2.68E+01	0.368	0
A,100,0	subsonic	AIR	18	1.11E+02	0	-0.101
A,100,0	sonic	AIR	18	2.39E+03	0	-0.472
A,100,0	subsonic	CWF	18	7.26E+01	-0.223	0
A,100,0	sonic	CWF	18	5.28E+01	-0.245	0
A,100,164	subsonic	AIR	19	2.70E+02	0	-0.187
A,100,164	sonic	AIR	19	5.69E+01	0	-0.013
A,100,164	subsonic	CWF	19	1.22E+02	-0.357	0
A,100,164	sonic	CWF	19	4.44E+01	0.191	0
A,240,100	subsonic	AIR	20	2.71E+02	0	-0.197
A,240,100	sonic	AIR	20	1.49E+03	0	-0.394
A,240,100	subsonic	CWF	20	7.72E+01	-0.164	0
A,240,100	sonic	CWF	20	5.06E+01	0.012	0
A,100,50	subsonic	AIR	20	2.08E+02	0	-0.165
A,100,50	sonic	AIR	20	1.47E+02	0	-0.131
A,100,50	subsonic	CWF	20	8.76E+01	-0.298	0
A,100,50	sonic	CWF	20	8.67E+01	-0.617	0
A,75,100	subsonic	AIR	21	1.72E+02	0	-0.151
A,75,100	sonic	AIR	21	4.99E+06	0	-1.352
A,75,100	subsonic	CWF	21	4.99E+01	0.097	0
A,75,100	sonic	CWF	21	3.77E+01	0.177	0

Table 8 Atomization Correlations

CWF	AIR VELOCITY	VARY	TEMP deg C	CONSTANT	1+1/ALR POWER	We POWER
B,100,100	subsonic	AIR	23	1.90E+02	0.000	-0.158
B,100,100	sonic	AIR	23	4.63E+03	0.000	-0.519
B,100,100	subsonic	AIR	60	7.03E+01	0.000	-0.035
B,100,100	sonic	AIR	60	1.49E+05	0.000	-0.926
B,100,100	subsonic	CWF	20	7.17E+01	-0.178	0.000
B,100,100	sonic	CWF	20	1.03E+02	-0.953	0.000
B,100,100	subsonic	CWF	55	6.40E+01	-0.127	0.000
B,100,100	sonic	CWF	55	4.59E+01	-0.139	0.000
B,100,260	subsonic	AIR	20	2.45E+02	0	-0.173
B,100,260	sonic	AIR	20	4.68E+01	0	0.019
B,100,260	subsonic	CWF	20	6.92E+01	0.008	0
B,100,260	sonic	CWF	20	5.30E+01	0.029	0.000
B,100,0	subsonic	AIR	20	1.78E+02	0	-0.155
B,100,0	sonic	AIR	20	3.22E+00	0	0.281
B,100,0	subsonic	CWF	20	1.96E+01	0.795	0
B,100,0	sonic	CWF	20	1.99E+01	0.789	0
B,75,100	subsonic	AIR	25	2.66E+02	0	-0.202
B,75,100	sonic	AIR	25	4.87E+03	0	-0.536
B,75,100	subsonic	CWF	25	7.72E+01	-0.233	0
B,75,100	sonic	CWF	25	7.94E+01	-0.618	0
B,200,100	subsonic	AIR	20	2.22E+02	0	-0.15
B,200,100	sonic	AIR	20	2.78E+02	0	-0.196
B,200,100	subsonic	CWF	20	8.33E+01	-0.222	0
B,200,100	sonic	CWF	20	5.36E+01	-0.062	0

Table 8 Atomization Correlations (Continued)

CWF	AIR VELOCITY	VARY	TEMP deg C	CONSTANT	1+1/ALR POWER	We POWER
C,100,100	subsonic	AIR	22	2.10E+02	0.000	-0.193
C,100,100	sonic	AIR	22	1.22E+04	0.000	-0.702
C,100,100	subsonic	AIR	55	1.29E+02	0.000	-0.129
C,100,100	sonic	AIR	55	1.27E+01	0.000	0.138
C,100,100	subsonic	CWF	20	5.42E+01	0.029	0.000
C,100,100	sonic	CWF	20	3.00E+01	0.434	0.000
C,100,100	subsonic	CWF	55	4.92E+01	0.104	0.000
C,100,100	sonic	CWF	55	4.55E+01	-0.179	0.000

CWF	AIR VELOCITY	VARY	TEMP deg C	CONSTANT	1+1/ALR POWER	We POWER
D,100,100	subsonic	AIR	20	2.22E+02	0	-0.167
D,100,100	sonic	AIR	20	1.37E+02	0	-0.118
D,100,100	subsonic	AIR	65	2.09E+02	0	-0.184
D,100,100	sonic	AIR	65	7.61E+05	0	-1.148
D,100,100	subsonic	CWF	20	1.00E+02	-0.327	0.000
D,100,100	sonic	CWF	20	5.18E+01	-0.094	0.000
D,100,100	subsonic	CWF	65	4.54E+01	0.114	0.000
D,100,100	sonic	CWF	65	5.52E+01	-0.219	0.000
D,100,150	subsonic	AIR	21	1.77E+02	0	-0.147
D,100,150	sonic	AIR	21	5.13E+04	0	-0.811
D,100,150	subsonic	CWF	23	9.68E+01	-0.346	0
D,100,150	sonic	CWF	23	4.96E+01	-0.049	0
D,100,50	subsonic	AIR	21	1.57E+02	0	-0.125
D,100,50	sonic	AIR	21	4.16E+03	0	-0.529
D,100,50	subsonic	CWF	21	9.55E+01	-0.295	0
D,100,50	sonic	CWF	21	5.78E+01	-0.163	0

Table 8 Atomization Correlations (Concluded)

The Weber number (We) used in the variable atomizing air flow rate tests was calculated as follows;

$$We = \frac{\rho \times Va^2 \times de}{\sigma} \qquad (4.8)$$

The dimensionless parameter We was chosen to correlate with the d3,2/Do data as it represents the balance between the aerodynamic drag of the atomizing air and the consolidating force of the CWF surface tension. The surface tension value, σ, used are those of the CWF as measured using the drop weight apparatus (Table 7).

Under variable CWF flow rate conditions the We is constant and the ALR was chosen to correlate with the d3,2/Do data.

4-3-2 Shake Down Tests

The initial testing was carried out to examine the performance of the NR atomizer. A schematic of the atomizer is shown in Figure 2. The mixing chamber gap width, atomizing air passage way cross section area, the axial and radial position of measurement of the spray PSD, the CWF flow rate and the atomization air flow rate were all varied to determine the most appropriate test matrix configuration.

The atomizer air post diameters were as follows;

Air Post Set	dal (m)
A	6.9E-3
B	7.5E-3
D	7.3E-3

Varying the air post diameter (dal) allowed the air delivery pressure (and density) to be varied independently of the air mass flow rate.

The spray PSD was measured at 15 and 20 cm axial distance from the atomizer tip. With air post A, the spray PSD was also measured at 25 cm axial distance. The axial distance was varied to determine the point where the atomization was complete and to insure that agglomeration of the drops had not started to occur. In each case noted above, data was collected at ALR and 0.5.

The spray drop PSD data is reported in the form of d3,2/Do, where d3,2 is the Sauter mean diameter and Do is given by;

$$Do = \frac{4 \times \text{wetted area}}{\text{wetted perimeter}} \qquad (4.9)$$

Parameters have been chosen such that Do = 0.89 cm and the dimensionless parameter d3,2/Do closely represents the Sauter mean diameter.

In virtually all cases, the spray PSD decreased as the ALR was increased regardless of the axial position, gap width, air channel cross section or the CWF flow rate.

Figures 6, 7, and 8 show the atomization data for air post set A at 2.3E kg/s CWF A flow and for mixing chamber gap widths of 6.1E-4, 7.6E-4 and 8.9E-4 meters respectively. The spray PSD did not increase as the gap width increased from 6.1E-4 to 7.6E-4 m, but did as the gap width was further increased to 8.9E-4 m. At CWF flows of 2.3E-2 kg/s and a gap width of 8.9E-4 m, the efficiency of transfer of the atomizing air to the CWF would be lower than at smaller gap widths and the spray PSD would increase. The atomization process seemed to be complete at axial distances less than 20 cm and did not either increase or decrease as the axial distance was varied.

Figures 9, 10 and 11 repeat the conditions seen in Figures 6, 7, and 8 with the CWF flow increased to 3.8E-2 kg/s. The increase in the CWF flow rate did not result in any particular change in the spray PSD other than to cause more variation in the data.

The test conditions seen in Figures 6 to 11 are repeated with air post B Figures 12 to 17. The most significant change was in the operational conditions that could be achieved. The maximum ALR achievable was reduced to 0.3 at the CWF flow of 3.8E-2 kg/s. As above, increasing the ALR, with these geometries, resulted in a decrease in the spray PSD. As the air passage cross section area is decreased, the same mass of air should be delivered at a higher density and lower velocity. The increase in the spray PSD from air post set A to set B indicates that the decrease in the air velocity contributes more to increasing the PSD than the increased density does to decreasing the PSD.

Air post set D data is shown in Figures 18 to 23. The air passage cross section area is less than set A and greater then set B. The trend from post set A to D was the same as the trend from set A to B, that is, the spray PSD was slightly greater owing to the reduced air velocity.

Based on effect of the atomizer geometries on the spray PSD and the operational parameters noted above, all of the subsequent spray testing carried out with a mixing chamber gap width of 7.6E-4 m and air post set A.

4-3-3 The Effect Of Additive Type And Amount On CWF Atomization

Four CWF configurations were tested with variations in the dispersant (d) and stabilizer (s) as depicted below;

A = d1,s1; B = d2,s1; C = d3,s1; D = d1,s2

The initial testing was carried out on the "Base Case" CWF configurations, which had the standard amount of the additives. The standard amount of the CWF additives is determined by the producer, CBDC, by examining the low shear rate rheology of the CWF.

4-3-3-1 A100,100, B100,100, C100,100, D100,100 AT 25 & 65°C

For each of the CWF's noted above, two sets of tests were conducted, one with variable atomizing air mass flow rate and one with variable CWF flow rate. Each of the test points were repeated once and the test groups carried out with the CWF temperature at ambient and raised to approximately 65°C. All of the variable air data was generated with a CWF flow of 2.3E-2 kg/s. The variable CWF flow rate data was collected with CWF flows of 2.3E-2, 3.2E-2, 3.8E-2 and 5.3E-2 kg/s.

CWF A100,100

The atomization data for CWF A100,100 is shown in Figures 24 to 27. The data is plotted in two groups on each graph, subsonic and sonic atomizer exit velocities.

For the variable air flow rate tests, the SMD of the spray droplet diameter decreased rapidly as the ALR was initially increased and then decreased with less dependence on the ALR. This trend is seen for all of the CWF configurations tested and reflects the equilibrium between the surface tension of the CWF droplets and the momentum of the atomizing air. Lane (6) has examined the equilibrium between liquid drops and air velocity and presents the following equation;

$$Cd \times 1/2 \times \rho \times Va^2 = 4 \times \sigma/d \qquad (4.10)$$

Equation 4.10 shows a power of 2 dependence of the drop diameter on the atomizing air velocity, which is approximately the trend shown in all of the figures showing variable air flow rate atomization data. Raising the CWF temperature to 55°C reduced the spray drop mean diameter.

When the atomizing air mass flow rate was held constant and the CWF varied, the data shown in Figures 26 and 27 was generated. During these tests, two sets of data were generated at a low and a high air flow rate with the same CWF flows. As was expected, the spray mean drop size decreased as the air mass flow rate was increased for any CWF flow rate. At 25°C, the spray drop size increased as the ALR was increased by

increasing the CWF flow rate at a fixed air mass flow rate. This implies that as the CWF flow is increased (decreased ALR) that the efficiency of transfer of the atomizing air energy is increasing. At 55°C, the trend at the subsonic conditions is the same as at 25°C and reverse of that seen at the sonic air velocity condition. The increase in the data scatter at sonic conditions and 55°C does not allow a true interpretation of the trends in this case.

CWF's B100,100, C100,100 and D100,100

The trends for CWF's B100,100, C100,100 and D100,100 are similar to those seen for CWF A100,100 for both variable air and CWF flow rates at 25 and 55°C. CWF B100,100 did have a more significant reduction in the spray mean drop size at low ALR values for the variable air flow data as the temperature was raised to 55°C.

Radial Position Data

Figures 40 to 43 show the radial positional data for CWF's A100,100, B100,100, C100,100 and D100,100 respectively. Each d3,2/Do value is comprised of the droplets seen as viewing through the spray at the radial distance indicated. The axial position is 20 cm from the atomzier. The maximum radial position has been determined by examining obscuration of the particle sizing laser. The edge of the spray was located in this manner when the laser obscuration was reduced to approximately 5%. An undetermined portion of the spray was at a radial position exceeding the maximum radial position measurement point. Data was collected with a CWF flow rate of 2.3E-2 kg/s and at ALR values of 0.3 and 0.9 (subsonic and sonic exit conditions respectively). In all cases the d3,2 increased with increasing radial distance from the spray axis and in all radial positions, the d3,2 decreased with increasing ALR. There was not a significant variation in the maximum radial distance of the spray pattern between the various CWF configurations. The data points shown in Figures 40 to 43 are the average of two measurements made at the same operational conditions.

Comparison of the CWF Configuration Atomization Data

Figure 44 shows a plot of the variation of the calculated d3,2/Do values from the A100,100 CWF configuration under variable atomizing air flow rate conditions. Differences of 5 μm or less should be considered to be insignificant in light of the accuracy of the spray drop size measurement and the goodness of the fit of the model equations. At subsonic conditions, CWF D100,100 does not atomize as well as the other configuration. At sonic conditions, CWF C100,100 atomizes slightly better at the highest ALR.

The variable CWF flow data (Figure 45) shows that CWF D100,100 atomized to produce a larger d3,2/Do at the lowest CWF flow rate (highest ALR) under subsonic air flow conditions and there wasn't any consistent trend at sonic conditions.

4-3-3-2 Variable Dispersant and Stabilizer Data

This section contains a discussion of the atomization data where both or either the dispersant and stabilizer type and amount have been varied.

CWF A Configuration Variation

- Vary Stabilizer, CWF A

Figures 46 to 51 show data where the concentration of the stabilizer s1 in the CWF A configuration has been varied for both vary air and vary CWF conditions. It would be expected that as the CWF stabilizer concentration was increased that the resistance to the deformation of the CWF during the atomization process would be increased as the viscosity of the CWF increased. This effect would then translate into the appearance of larger drops in the spray and a larger d3,2/Do value. The trends of d3,2/Do versus ALR for the vary air and CWF flow rate conditions are similar to those for the base case CWF configuration. Figure 61 shows the variation of the calculated d3,2/Do values, for the variable stabilizer CWF A configurations, from the A100,100 calculated values. The trends are as would be expected, that is as the stabilizer amount is increased, the atomization performance decreases. The water content of CWF A100,0 was approximately 3% lower than the other variable stabilizer CWF A configurations (A100,100, A100,50 and A100,164). During the atomization of a CWF, some of the water in the CWF may be stripped from the coal in the CWF and produce very small drops. The atomization of CWF A100,0 is improved over that of the higher stabilizer concentration configurations despite the potentially negative effect of the lower water content. Figure 3 shows the coal PSD information for the A configuration CWF's. The most variation in the coal PSD is seen in CWF A100,0 which may further affect the atomization.

During the initial stages of the atomization process the formation of relatively large drops may be effected by the surface tension of the bulk CWF. The surface tension data in Table 7 shows that the surface tension of the CWF, as measured by both the ring and drop methods, increases as the stabilizer concentration is increased. This data may not accurately represent the true surface tension of the CWF surface due to the effect of the long chain dispersant molecule. The dispersant may adhere to the ring in the ring method, and resist the separation of the drop in the drop method. In both cases the surface tension data would be erroneously effected. Theoretically, the surface tension of the CWF should be decreased due to the presence of the coal and the stabilizer. Therefore as the stabilizer concentration is increased, the surface tension

resistance or equilibrium condition should result in smaller drops being formed. The high viscosity of the CWF will have a much greater effect during the initial drop formation stage and negate any variation in the surface tension.

• Vary Dispersant, CWF A

The effect of varying the CWF A dispersant, dl, amount is shown in Figures 52 to 55. The dispersant allows the hydrophobic surface of the coal to be wetted and a slurry of high coal content to be made. During the atomization process, the initial stages of the drop formation process involves the deformation of the CWF by the atomizer into thin sheets. As the high velocity atomizing air passes over the CWF, disturbances in the sheet surface are amplified to a point where a portion of the CWF leaves the bulk flow. This portion can be in the form of a ligament or a drop. The ligaments are broken down further by the aerodynamic action of the atomizing air. The surface tension of the surface of the CWF ligament will initially resist the deformation as dilational distortions are formed. When the ligament becomes unstable it will disintegrate into drops and the surface tension of the CWF surface will form the drops into spheres. The subsequent disintegration of the CWF drops into smaller drops will reach an equilibrium between the surface tension forces in the CWF and the aerodynamic force of the atomizing air (see equation 4.9). As the disintegration of the CWF continues and smaller drops are formed the size of the coal particles in the CWF will become significant in relation to the drop size formed. At this point, the cleavage of the drops will take place at the coal/water interface. Cleavage of larger drops will involve separation at both the coal/water interface and in the liquid phase only. The dynamic process of surface tension formation in relation to the drop formation time (ref ???/) would result in the surface tension of the liquid phase being that of water. The interfacial surface tension of the coal and water will play a more significant role as the drop size decreases and more of the cleavage takes place at the coal/water interface. The addition of a dispersant will reduce the interfacial surface tension between the coal and water and resist the drop formation process. The coal/water interfacial surface tension of the multi-phase CWF's has the opposite effect on the atomization process than that seen in a single phase liquid during the formation of the micron size drops. In consideration of the above, the addition of any amount of dispersant that reduces the coal/water surface tension should result in larger drop sizes being formed. This will be discussed below. The atomization trends for CWF's A240,100 and A75,100 are similar to those seen for the other CWF configurations.

• Comparison of CWF A's to CWF A100,100

Figure 62 shows the deviation of the calculated d3,2/Do values from the calculated A100,100 data. Reducing the dispersant concentration to 75% had an insignificant effect on the atomization at low ALR values and

showed some improvement at the highest ALR conditions. Increasing the dispersant concentration to 240% caused an increase in the d3,2/Do value of 15 (17 μm) at the lowest ALR with the difference decreasing as the ALR increased. Under variable CWF flow rate conditions (Figure 63), the trends were less clear.

CWF B Configuration Additive Variation

• Vary Stabilizer, CWF B

CWF B contained the dispersant d2 and the same stabilizer, s1, as CWF A.

The effect of varying the stabilizer s1 in conjunction with a different dispersant, d2, is shown in Figures 65 to 68. Figure 65, for CWF B100,0 can be compared to the data in Figure 46 for CWF A100,0. It appears that the dispersant d2, which apparently meets the producers requirements for a satisfactory CWF, has less of a detrimental effect on the CWF atomization at low ALR conditions when a stabilizer is not present. Referring to Figure 44, it can seen that there is no difference in the atomization of the CWF A and B when the stabilizer is present at 100% concentration. Table 7 shows the effect of varying the stabilizer concentration of the CWF surface tension. The overall trend is for the CWF surface tension to increase as the stabilizer concentration is increased. This slight increase in the surface tension would resist the formation of the larger drops, where the bulk CWF surface tension would play a role, but would be insignificant in comparison to the viscosity effect.

When the flow rate of CWF B is varied at constant air flow, Figure 66, the trend at the low air is significantly different than that encountered in the other CWF configurations. The atomization performance deteriorates rapidly as the CWF flow is increased.

When the concentration of stabilizer s1 was increased in conjunction with dispersant d2 (Figures 67 and 68), the effect was similar to that seen for the CWF A configuration (Figures 50 and 51).

• Vary Dispersant, CWF B

The effect of varying the dispersant d2 amount can be seen in Figures 69 and 70 for CWF B200,100 and Figures 71 and 72 for CWF B75,100. As the dispersant d2 concentration was increased, the spray SMD increased. The radial position spray data for the variable additive concentrations of CWF B are shown in Figures 73 to 76. Increasing the dispersant d2 concentration caused the angle of the spray to increase as seen in Figure 75.

• Comparison of CWF B's to B100,100

Comparisons of the CWF B configuration calculated atomization data to the B100,100 CWF are shown in Figures 77 to 80. While varying the atomizing air flow rate, decreasing the dispersant d2 to 75 percent of normal had little effect. This may be as a result of the lower water content of CWF B75,100. Lowering the water content results in less water being atomized and making less contribution to the smaller drop size fraction. Increasing dispersant d2 to 200 percent of normal resulted in a significant increase in the spray d3,2/Do despite any advantage that the higher water content may have given to CWF B200,100.

CWF D Configuration Additive Variation

• Vary stabilizer, CWF D

The measured and calculated d3,2/Do data for CWF's D100,50 and D100,150 are shown in Figures 81 to 84. The trends for these CWF's is similar to that seen in the other configurations for both vary air and CWF flow rate operations. Radial position data is shown in Figures 85 and 86.

• Comparison of CWF D's to D100,100

Figures 87 and 88 show the comparison of the calculated d3,2/Do to the D100,100 CWF for the vary air and CWF flow conditions respectively. During the variable air mass flow rate tests, the variation in stabilizer s2 in combination with dispersant d1 did not produce the results expected. At low ALR both the increased and decreased stabilizer concentration CWF's produced a smaller mean drop size. It would be expected that the D100,50 would produce smaller and the D100,150 larger drops, especially at the lower ALR conditions. Examination of the low and high shear rate rheology data shows that both the D100,50 and D100,150 had lower viscosities than the D100,100. The result for the D100,50 is expected while the D100,50 rheology is not, especially considering that the water content of the D100,150 was nearly two percent lower than that of the D100,100. Figure 5 shows that the coal PSD for both the D100,50 and D100,150 were the same and both were different than the D100,100, especially in the larger size ranges. The coal PSD may have effected both the rheology and the atomization. Table 5 shows that the dynamic yield stress of CWF D100,100 is higher than the other CWF D configurations.

4-4 INSTRUMENTED ATOMIZER DATA

The atomizer shown in Figure 2 was modified as shown in Photo 3 to allow the measurement of the static pressure in the atomizing air passage way and the mixing chamber. The atomizing air passage pressure was measured at the inside wall of the air passage just prior to the entrance to the mixing chamber. The mixing chamber pressure was measured at the midpoint of the mixing chamber length on the ring side.

As with the other atomization tests, the atomizer was operated with fixed liquid flow rate and variable air flow and vice versa. Pressure measurements were made with CWF A100,100 and also city tap water. The operational data is shown in Table ?? in appendix A. Figure 89 shows the mixing chamber pressure versus the air mass flow rate for CWF and water at 2.3E-2 kg/s operation. When water is being atomized, the static pressure in the mixing chamber remains negative until an air mass flow rate of approximately 0.023 kg/s is reached. When atomizing CWF, the mixing chamber pressure is approximately ambient until an air flow rate of 0.016 kg/s is reached.

When the air mass flow rate is held constant and the liquid flow rate varied the mixing chamber pressure increases almost linearly as the liquid mass flow rate is increased. Figure 90 shows data for CWF and for water at two air mass flow rates each. The mixing chamber pressure is less for water operation at low water flow rates and exceeds the low CWF flow mixing chamber pressure. With high air flow rates the mixing chamber pressure during CWF atomization is always higher than the water atomization pressures.

The alignment of the cone and ring in the atomizer is shown in the operational data tables. It was observed that the alignment of the mixing chamber parts had a significant effect on the mixing chamber pressure.

5. CONCLUSIONS

5-1 CWF DATA

Analysis of the CWF's included low shear rate, high shear rate and yield stress rheology tests, surface tension of both the CWF and it's filtrate using ring and drop methods and coal particle size distribution.

Variations are seen in the CWF production parameters, such as ash, density and moisture, which are within the accepted limits of the CWF production. These variations can have a significant effect on the CWF analysis results. Trends in the analysis noted above were not always consistent and in some cases could not be explained with the data available.

Low Shear Rate Rheology

Increasing the concentration of any of the stabilizers resulted in an increase in the low shear rate viscosity. Variations in the CWF water content effected these results. Anomalies were seen in the CWF D configurations which could not be explained by any of the other analysis.

Increasing the CWF dispersant concentration resulted in an increase in the low shear rate viscosity for the two dispersants tested.

Yield Stress

Generally the yield stresses increased as the stabilizer concentration was increased for all stabilizers. As for the low shear rate viscosity, the CWF D configuration showed unexplainable anomalies in the data trends.

Increasing the dispersant concentration caused an increase in the yield stress in most cases.

High Shear Rate Rheology

The high shear rate (ie 10,000 s^{-1}) viscosity trends when increasing the stabilizer concentration were the same as seen at low shear rates.

Increasing the dispersant concentration resulted in lower high shear rate viscosities initially and had no effect as the concentration was increased.

Surface Tension

Increased concentrations of dispersant d1 (with stabilizer s1, CWF A) resulted in a decrease in the measured surface tension of the CWF and filtrate as determined with both the ring and drop methods. As the concentration of dispersant d2 (with stabilizer s2, CWF B) was increased the surface tension decreased then increased as determined by both methods for both the CWF and filtrate.

The highest concentrations of stabilizer s1 caused an increase in the measured surface tension of the CWF and filtrate when combined with dispersants d1 and d2 (CWF's A and B respectively). Increasing the concentration of stabilizer s2 with dispersant d1 (CWF D) resulted in a continuous decrease in the surface tension.

Coal Particle Size Distribution

Significant variations in the coal particle size distribution (PSD) data were seen. The variations were in the large size range for some of the CWF's and small size range for others. The effect of these variations on the CWF atomization have not been investigated completely.

5-2 ATOMIZATION DATA

A total of fifteen combinations of various concentrations of three dispersants and two stabilizers were atomized. Atomization was carried out with variable air and CWF flow rates at ambient and raised CWF temperatures.

The dispersant and stabilizer combinations were as follows;

A = d1,s1 B = d2,s1 C = d3,s1 D = d1,s2

The CWF's tested are noted below, where the numbers indicate the percentage of the normal dispersant and stabilizer amounts used;

A,100,0	B,100,0
A,100,100	B,100,100
A,100,169	B,100,260
A,100,50	B,200,100
A,240,100	B,75,100
A,75,100	
C,100,100	D,100,100
	D,100,150
	D,100,50

The measured data were correlated with appropriate parameters using multiple linear regression. The calculated data was then used to compare the effect of the chemical type and amount on the atomization of the CWF's.

When examining the base case CWF configurations (100,100 concentrations), CWF D atomized to form larger droplets than the other CWF's.

Variable Dispersant Effect on Atomization

The spray droplet mean size increased with increasing dispersant concentration and decreased with decreasing concentration for both CWF's A and B. The magnitude of the variation decreased as the atomizing air to CWF mass flow rate (ALR) increased.

Variable Stabilizer Effect on Atomization

The same relative effects were seen for variations in the stabilizer concentration for CWF's A and B as were seen in the variable dispersant data. As with the majority of the other analysis carried out on CWF D, the atomization data did not follow the expected trends and cannot be explained by the analysis carried out in this work.

5-3 INSTRUMENTED ATOMIZER PRESSURES

Preliminary data was collected with an atomizer where the mixing chamber and atomizing air pressures were measured. The mixing chamber pressure showed a high sensitivity to the alignment of the cone in the atomizer (effecting the mixing chamber gap with).

ACKNOWLEDGEMENTS

Funding for this project was provided from the Cape Breton Development Corporation (CBDC) (50%) and Energy Mines and Resources Canada (50%) through the Department of Supply and Services (DSS) Canada 50/50 Cost Shared Program.

The CBDC produced the various coal-water fuel (CWF) configurations tested in the project and provided analysis of the CWF used in this report.

Mr. Larry Giffin carried out the CWF analysis and atomization testing reported on herein.

Dr. Kelly Thambimuthu was the Scientific Authority for DSS and provided assistance in test matrix development and data analysis.

REFERENCES

(1) Warchol,J.J., Vecci,S.J., "Coal-Water-Slurry Evaluation", Volume 1: Revised Laboratory Test Standards, EPRI CS-3413, July 1985

(2) York,J.L., Stubbs,H.E, Tek,M.R., "The Mechanism of Disintergration of Liquid Sheets", Transactions of the ASME, VOL 75 (1953)

(3) Rayleigh, Lord, "On the Instability of Jets", Proc. Lond. math. Soc. VOL 10 (1878) No. 4

(4) Addison,C.C., J. chem. Soc. VOL 5 (1943) No. 35

(5) Dombrowski,N., Chapter 16, "Spray Drying", in "Biomedical and Biological Engineering Science", ed Blakebrough,N., VOL 2 (1968), Acadamic Press, London

(6) Lane,W.R., "Shatter of Drops in Streams of Air", Industrial and Engineering Chemistry, VOL 43 (1951) NO 6, pp 1312-1317

(7) Funk,J.E., Dinger,D.R., Funk Jr.,J.E., "Coal Grinding and Particle Size Distribution Studies for Coal-Water Slurries at High Solids Content", Final Report, Empire Electric Energy Research Corporation, (1980), 129p

Photo 1 CWF A100,100, 3.2E-2 kg/s, ALR = 0.19

Photo 2 CWF B100,240, 3.2E-2 kg/s, ARL = 0.19

Photo 3 Instrumented NRCC Atomizer

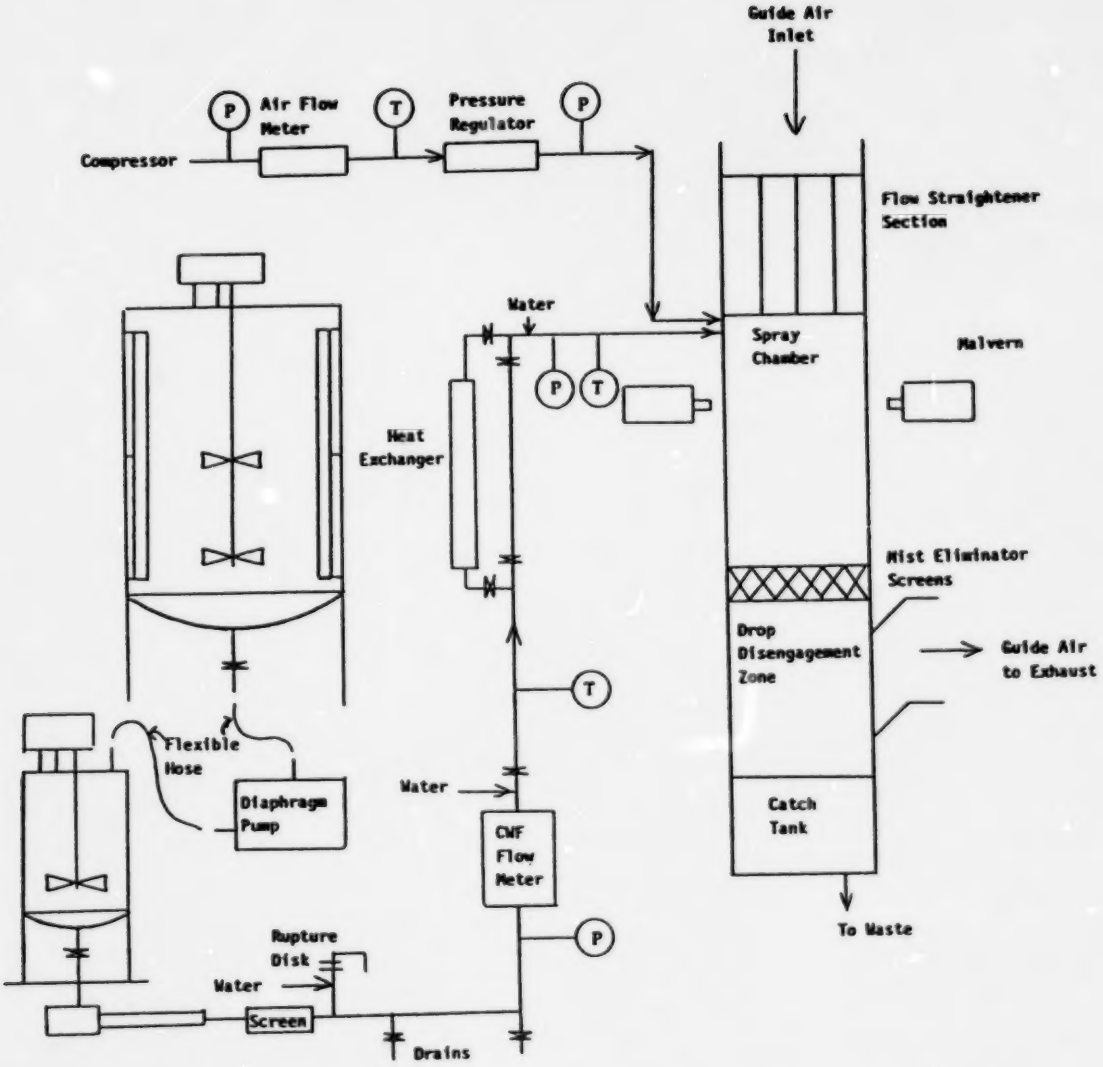

Figure 1 Schematic of the NSRFC CWF Atomization Test Facility

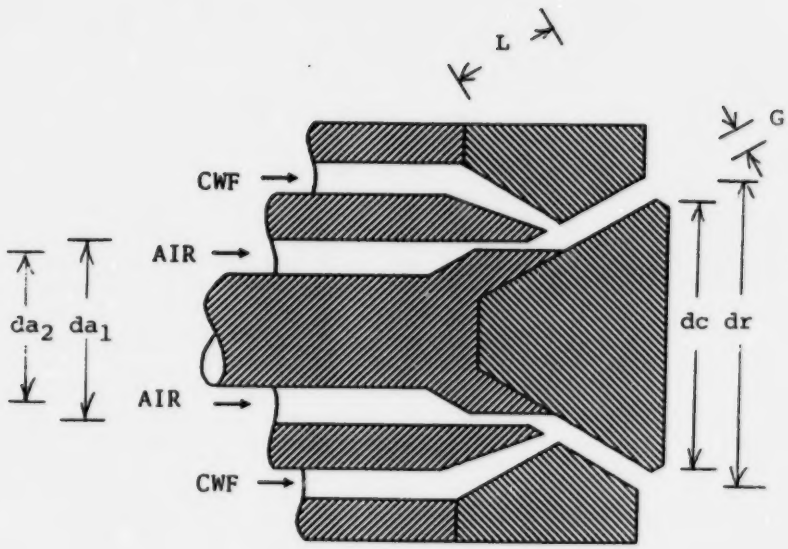

Figure 2 Schematic of the NRC CWF Atomizer

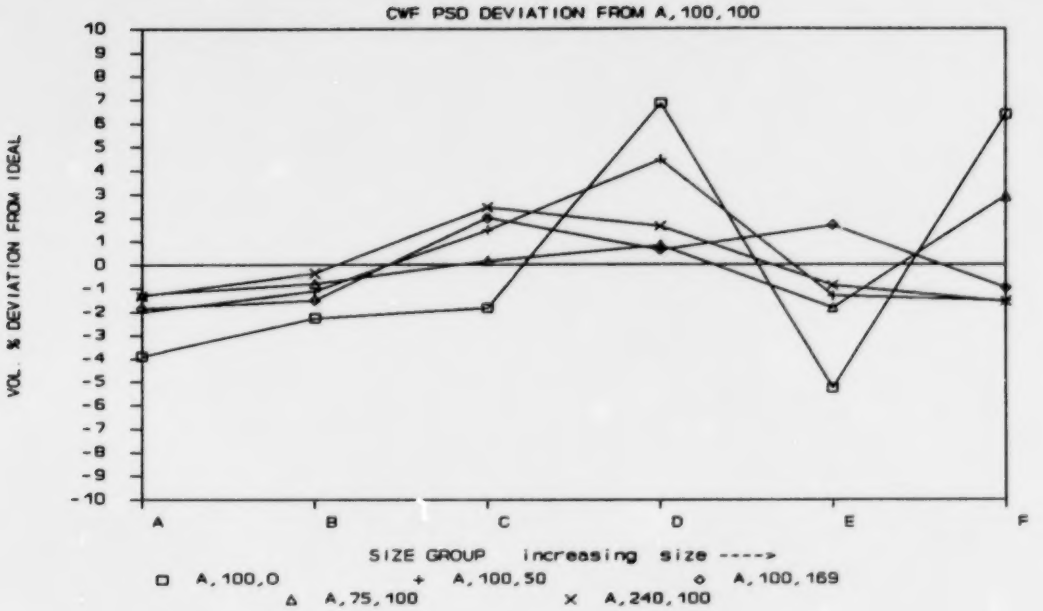

Figure 3 CWF A, Variation of PSD From A,100,100

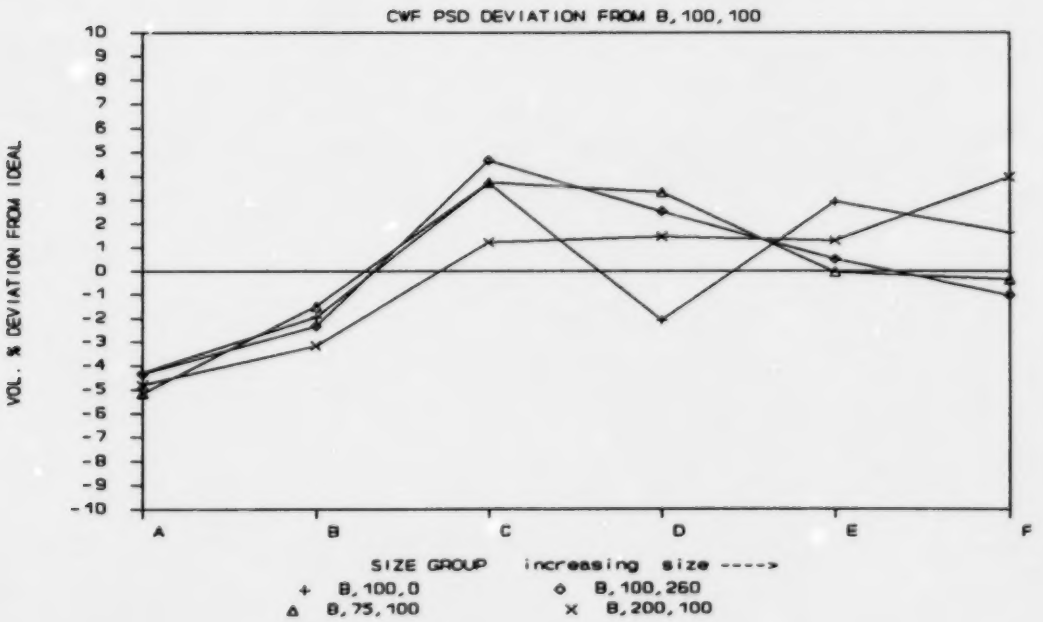

Figure 4 CWF B, Variation of PSD From B,100,100

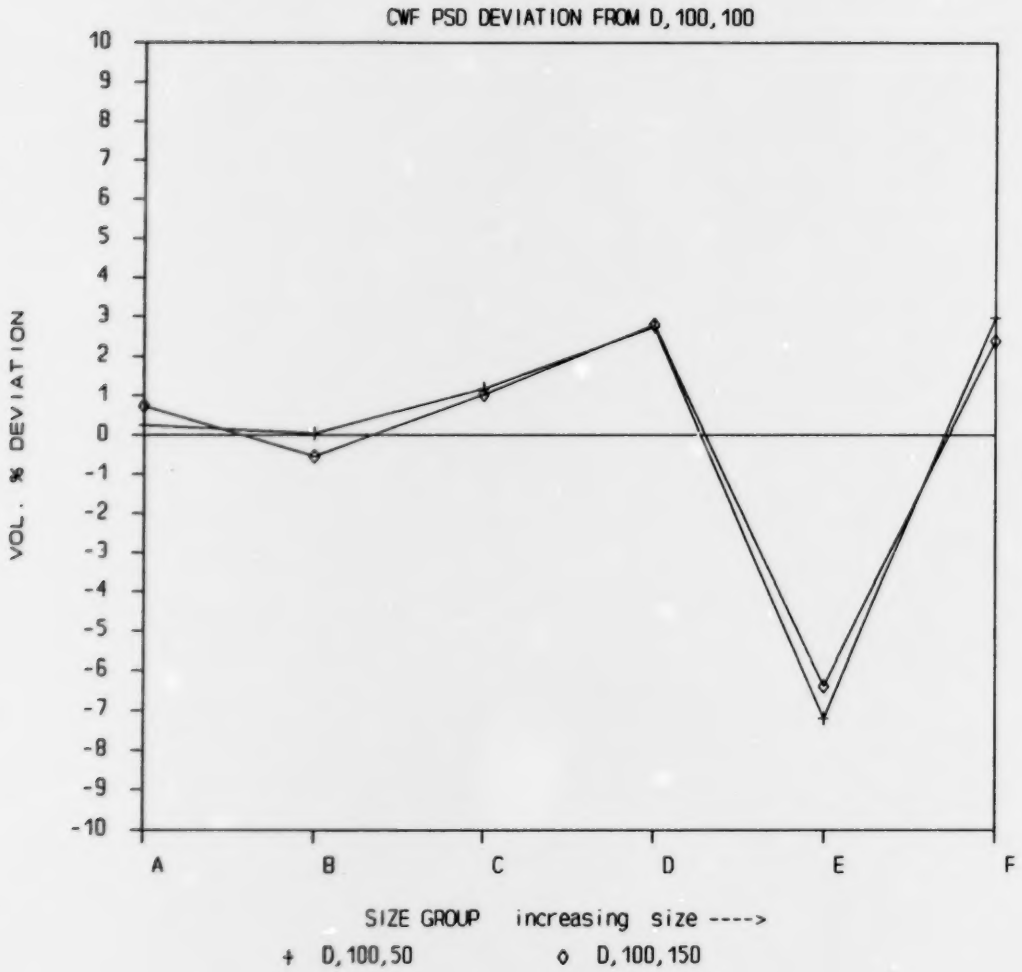

Figure 5 CWF D, Variation of PSD From D,100,100

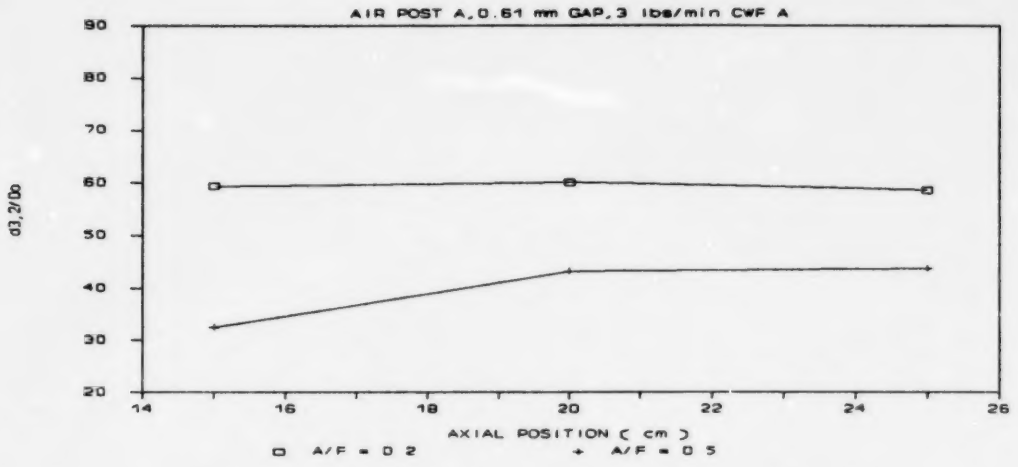

Figure 6 Air Post Set A, CWF A, Mixing Chamber GAP 0.61 mm, 3 lbs

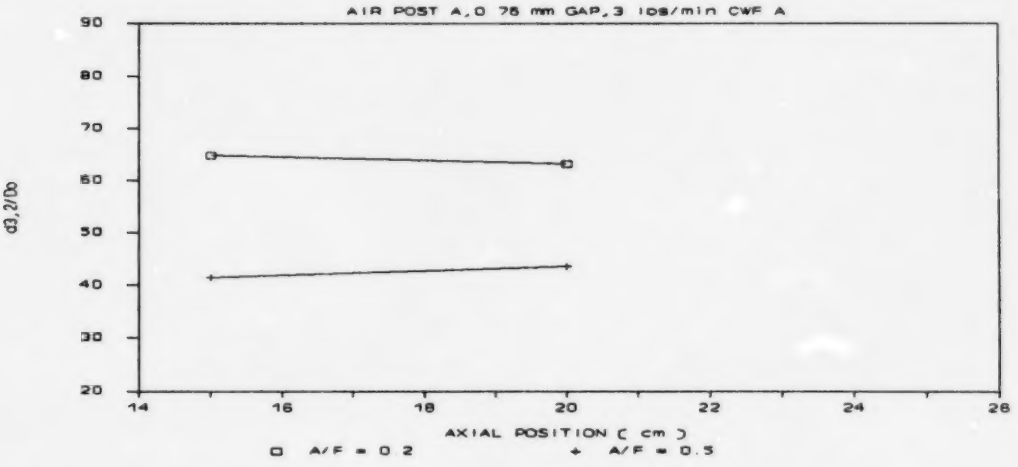

Figure 7 Air Post Set A, CWF A, Mixing Chamber GAP 0.76 mm, 3 lbs

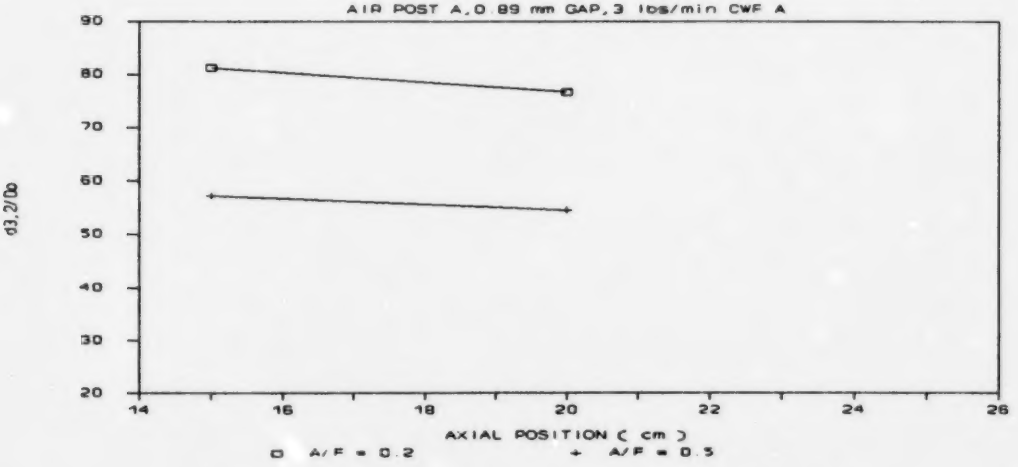

Figure 8 Air Post Set A, CWF A, Mixing Chamber GAP 0.89 mm, 3 lbs

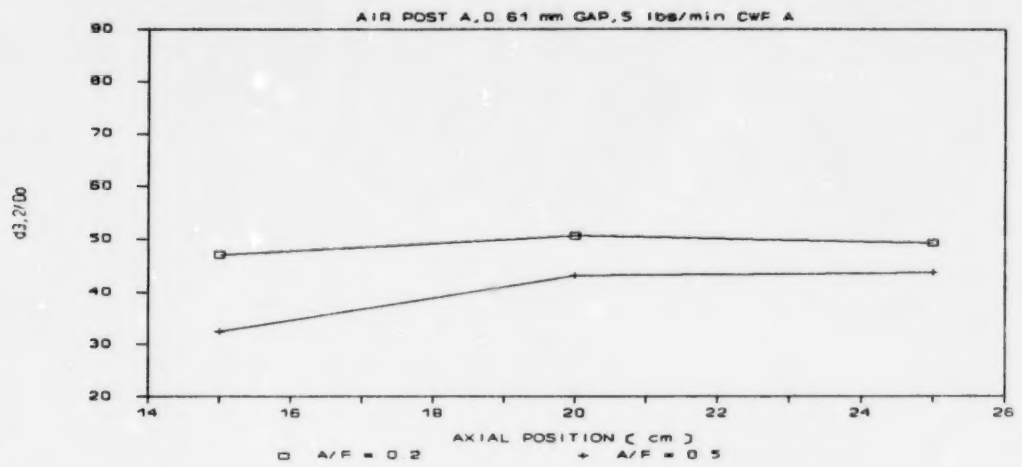

Figure 9 Air Post Set A, CWF A, Mixing Chamber GAP 0.61 mm, 5 lbs

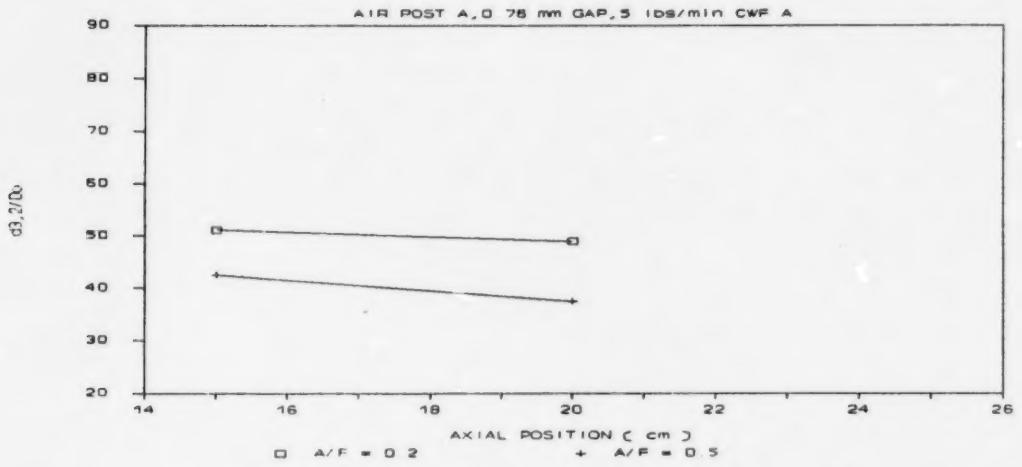

Figure 10 Air Post Set A, CWF A, Mixing Chamber GAP 0.76 mm, 5 lbs

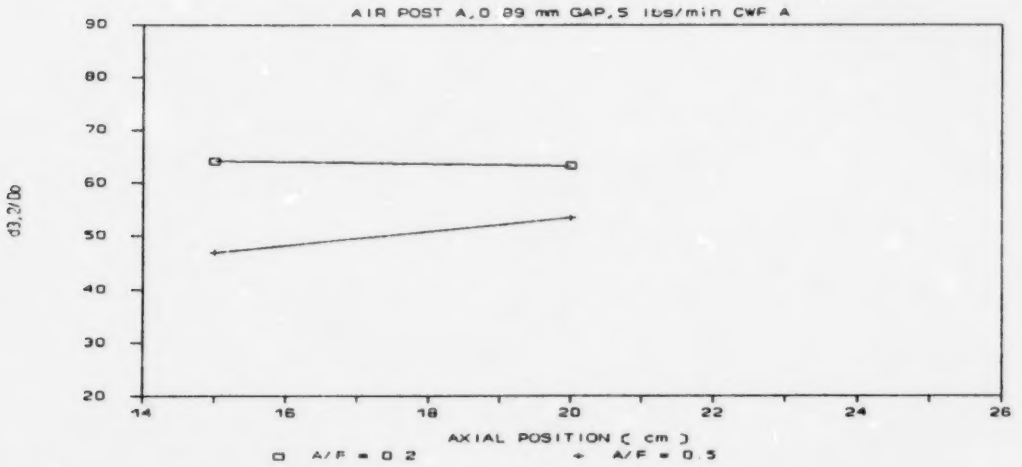

Figure 11 Air Post Set A, CWF A, Mixing Chamber GAP 0.89 mm, 5 lbs

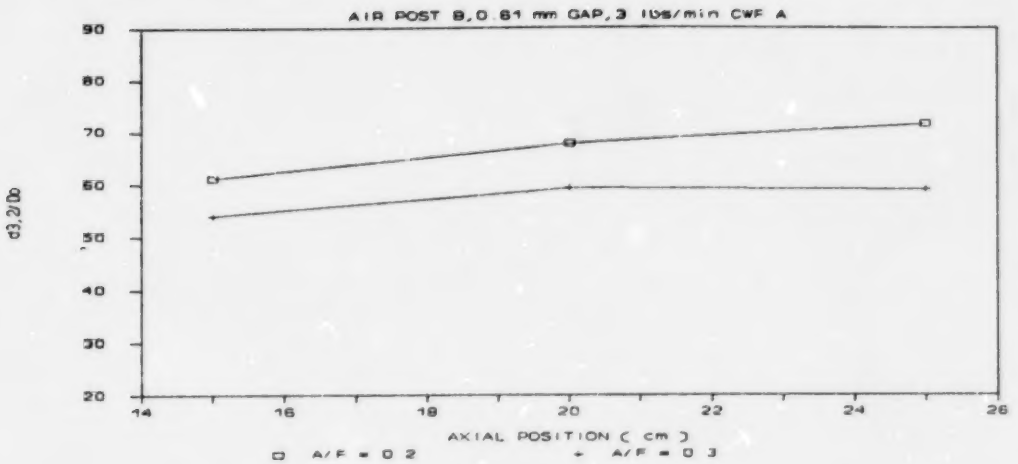

Figure 12 Air Post Set B, CWF A, Mixing Chamber GAP 0.61 mm, 3 lbs

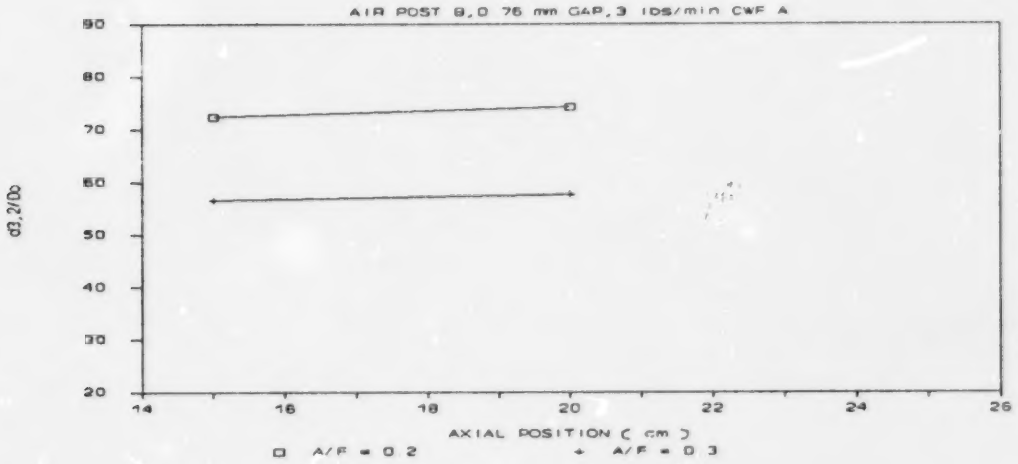

Figure 13 Air Post Set B, CWF A, Mixing Chamber GAP 0.76 mm, 3 lbs

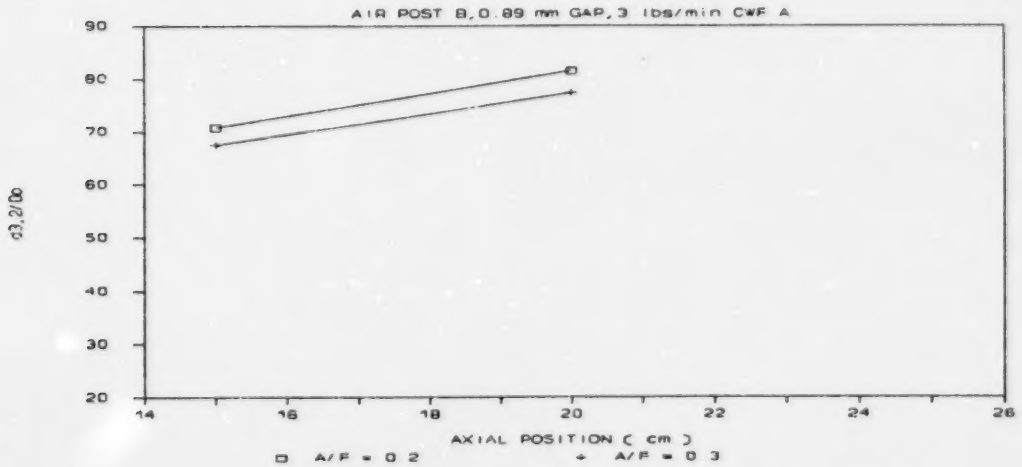

Figure 14 Air Post Set B, CWF A, Mixing Chamber GAP 0.89 mm, 3 lbs

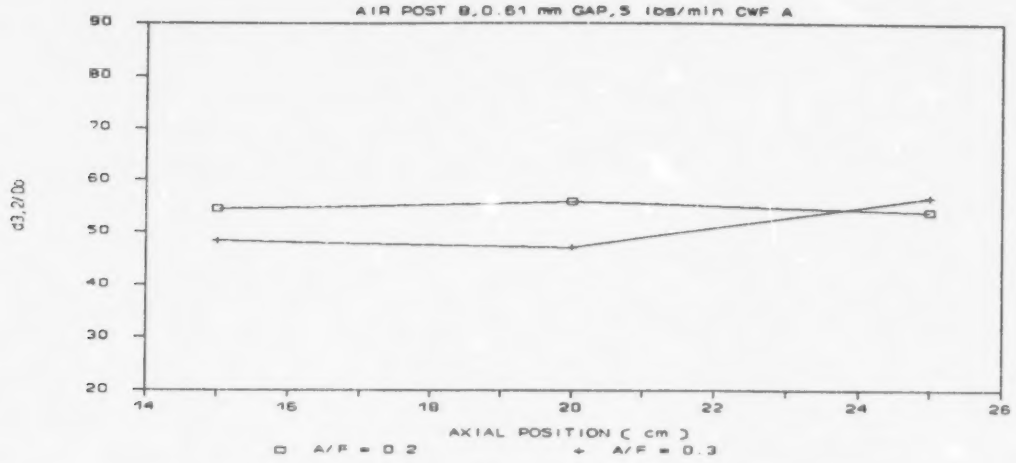

Figure 15 Air Post Set B, CWF A, Mixing Chamber GAP 0.61 mm, 5 lbs

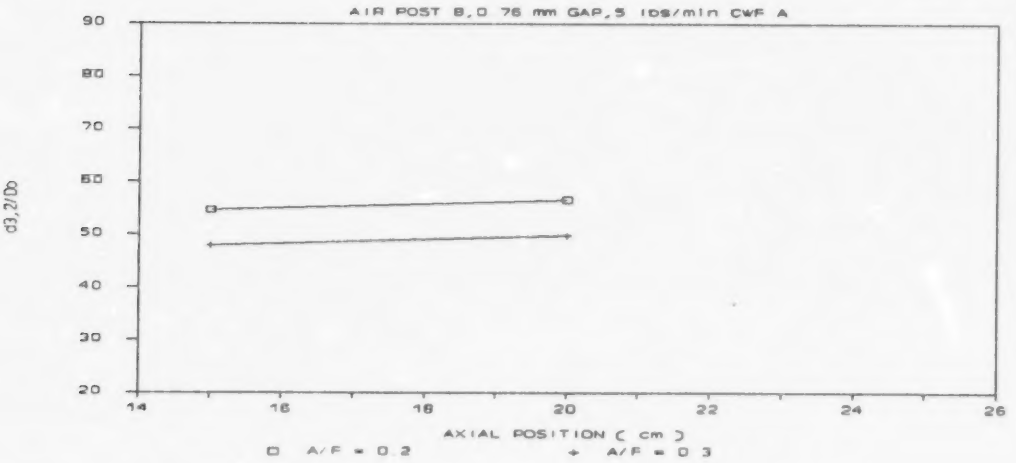

Figure 16 Air Post Set B, CWF A, Mixing Chamber GAP 0.76 mm, 5 lbs

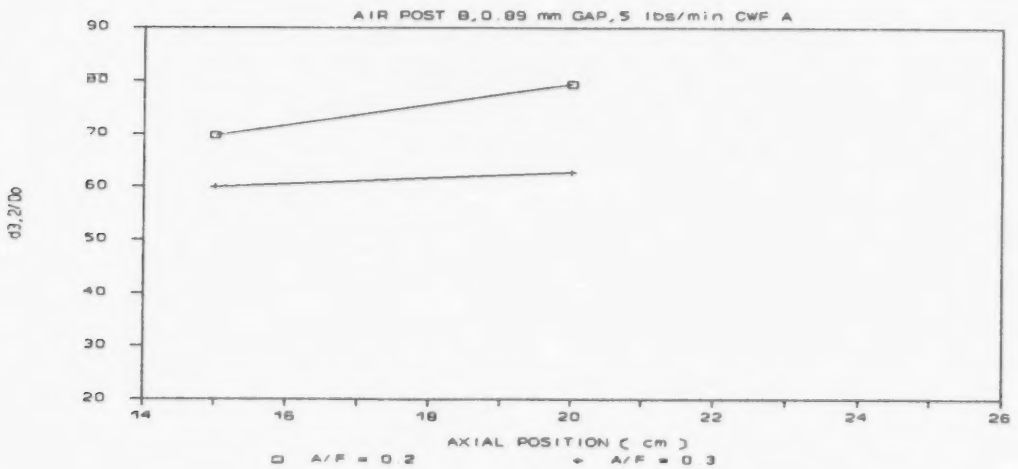

Figure 17 Air Post Set B, CWF A, Mixing Chamber GAP 0.89 mm, 5 lbs

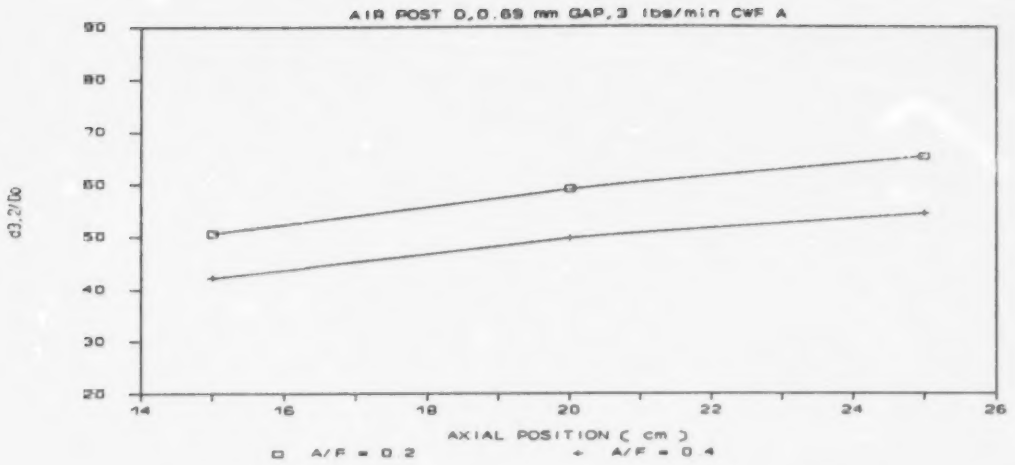

Figure 18 Air Post Set D, CWF A, Mixing Chamber GAP 0.61 mm, 3 lbs

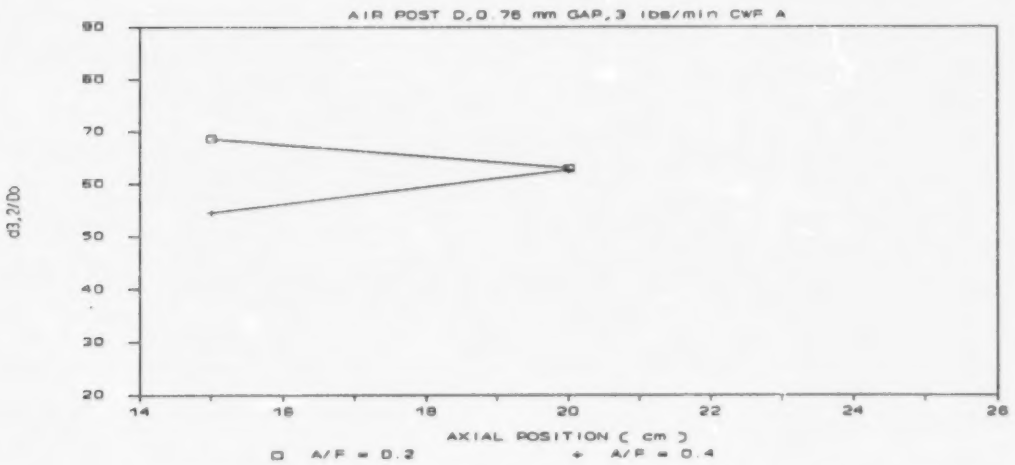

Figure 19 Air Post Set D, CWF A, Mixing Chamber GAP 0.76 mm, 3 lbs

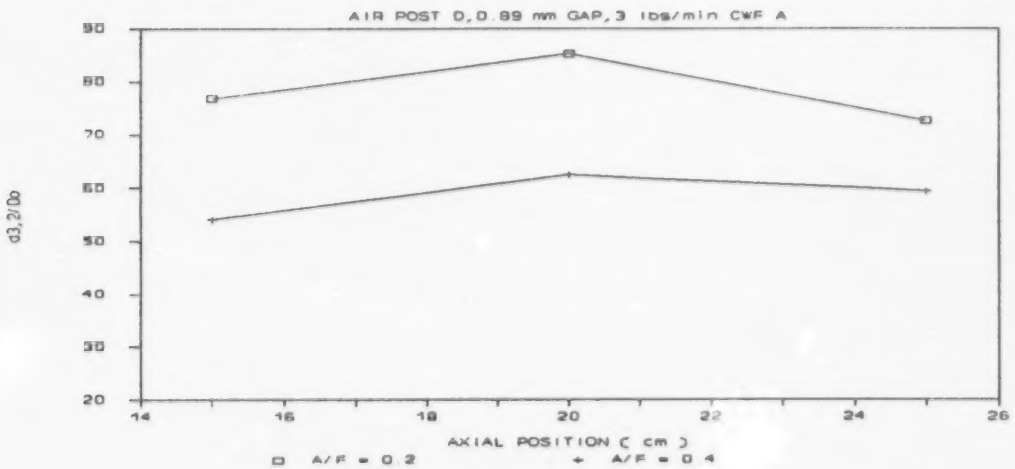

Figure 20 Air Post Set D, CWF A, Mixing Chamber GAP 0.89 mm, 3 lbs

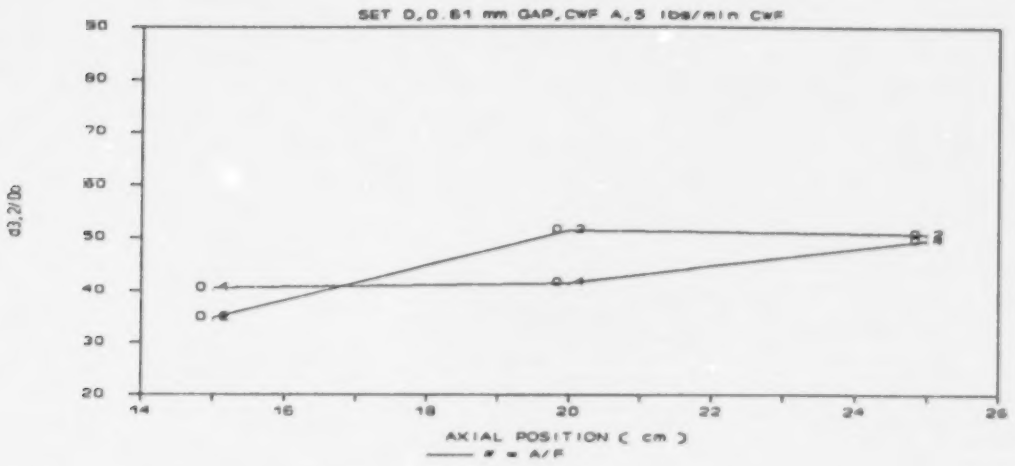

Figure 21 Air Post Set D, CWF A, Mixing Chamber GAP 0.61 mm, 5 lbs

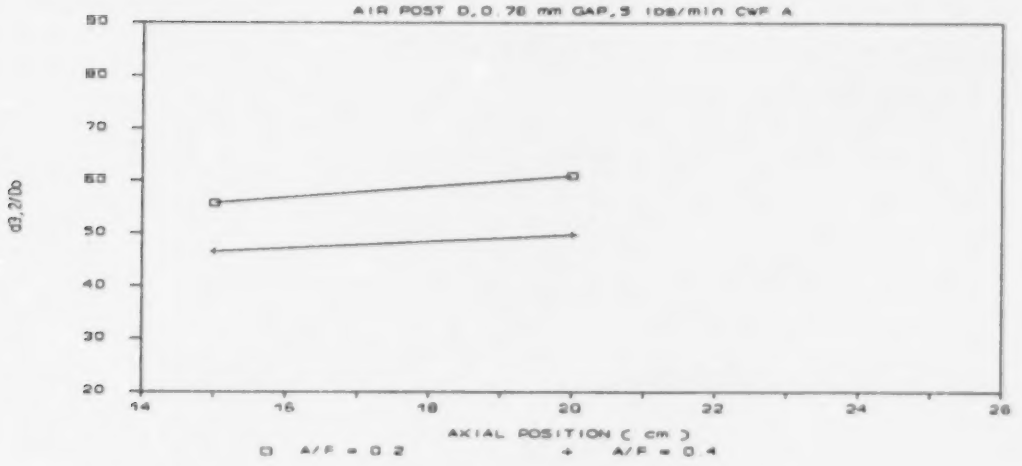

Figure 22 Air Post Set D, CWF A, Mixing Chamber GAP 0.76 mm, 5 lbs

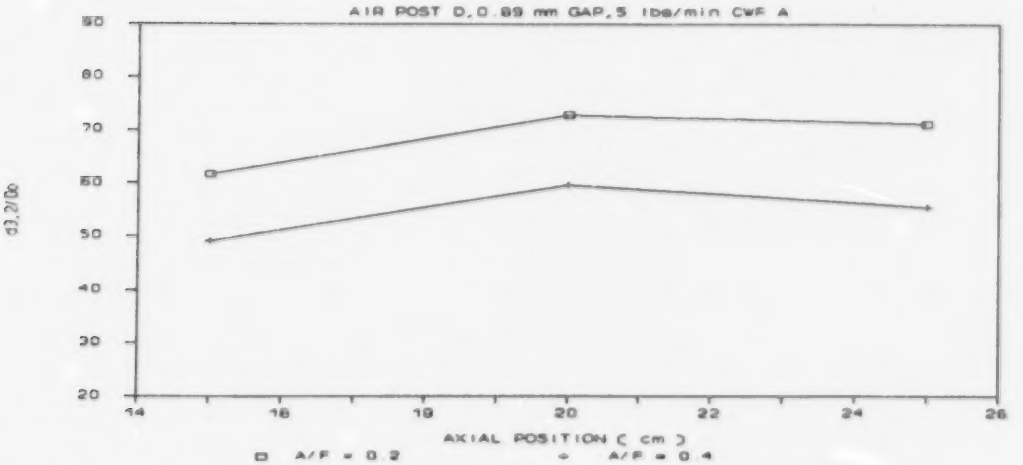

Figure 23 Air Post Set D, CWF A, Mixing Chamber GAP 0.89 mm, 5 lbs

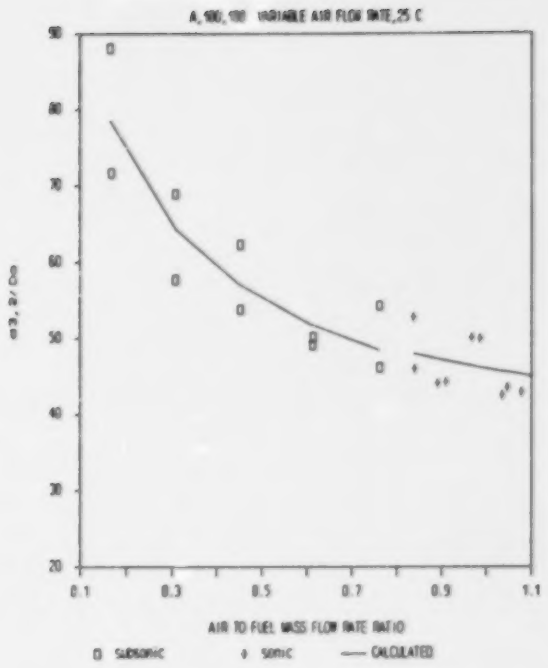

Figure 24 A,100,100, Variable Air Flow Rate d3,2/Do Versus A/F at 25°C

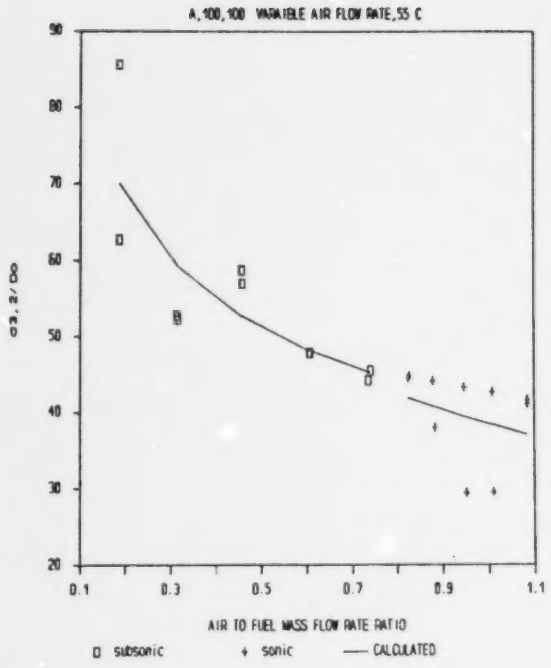

Figure 25 A,100,100, Variable Air Flow Rate d3,2/Do Versus A/F at 55°C

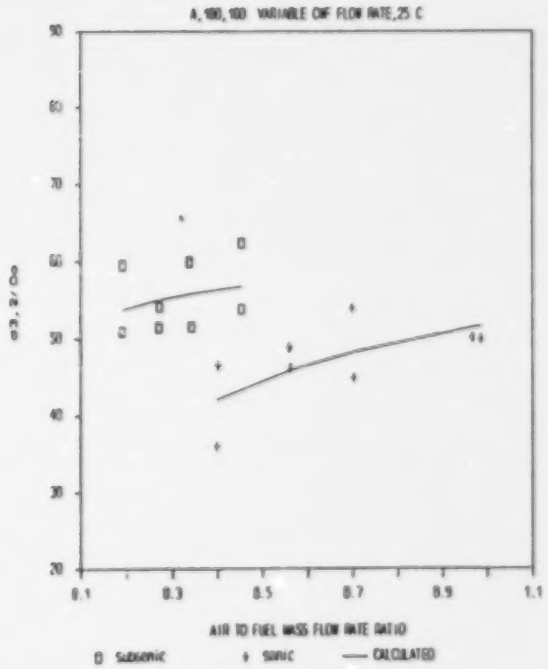

Figure 26 A,100,100, Variable CWF Flow Rate d3,2/Do Versus A/F at 25°C

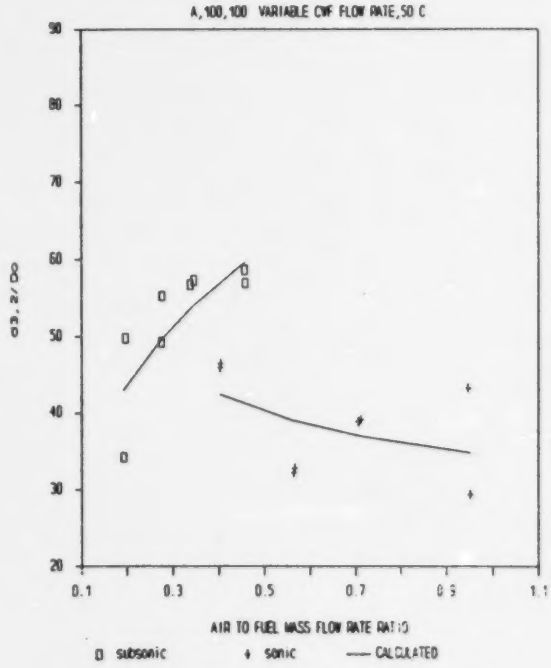

Figure 27 A,100,100, Variable CWF Flow Rate d3,2/Do Versus A/F at 50°C

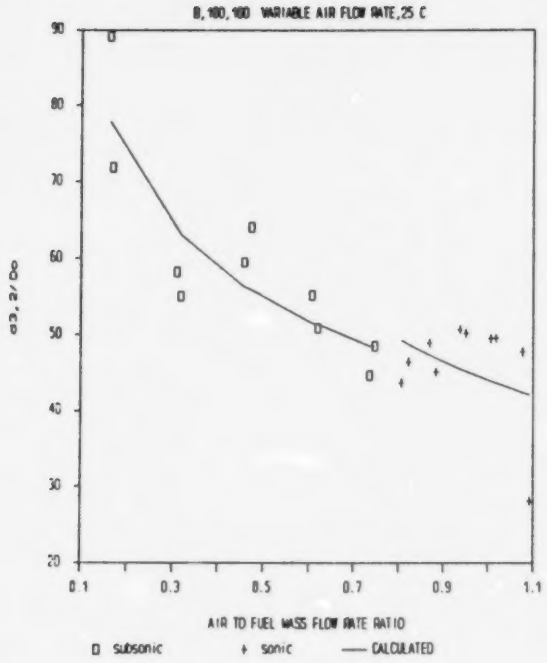

Figure 28 B,100,100, Variable Air Flow Rate
d3,2/Do Versus A/F at 25°C

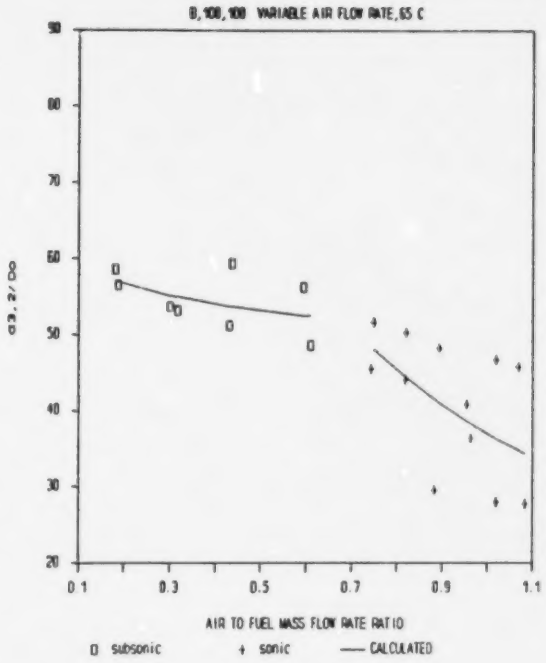

Figure 29 B,100,100, Variable Air Flow Rate
d3,2/Do Versus A/F at 65°C

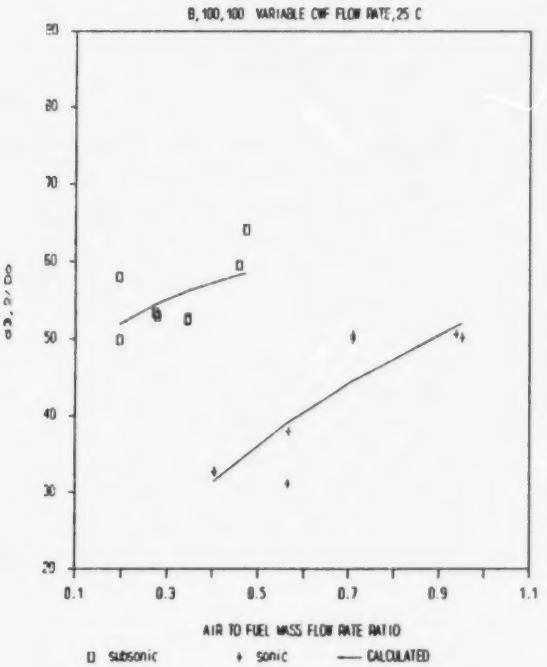

Figure 30 B,100,100, Variable CWF Flow Rate
d3,2/Do Versus A/F at 25°C

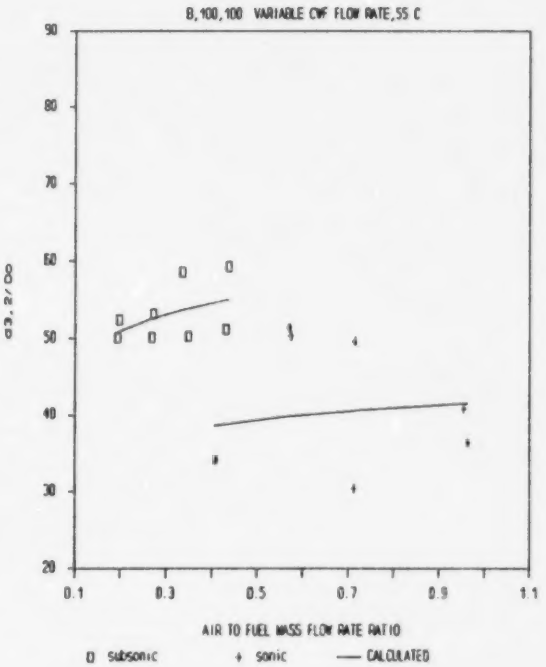

Figure 31 B,100,100, Variable CWF Flow Rate
d3,2/Do Versus A/F at 55°C

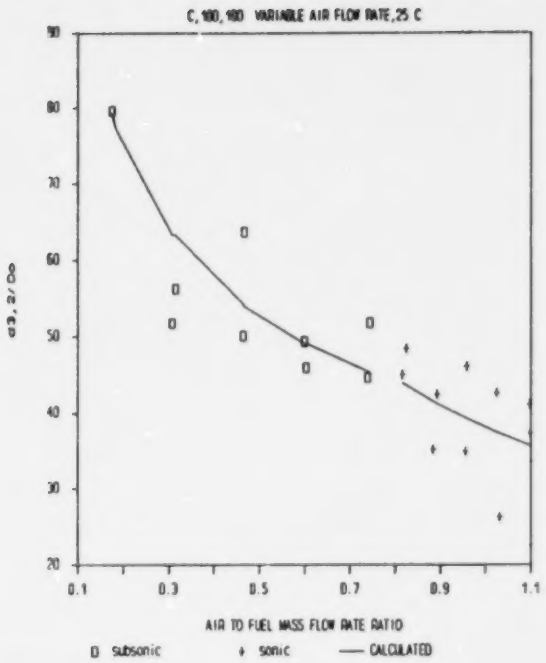

Figure 32 C,100,100, Variable Air Flow Rate d3,2/Do Versus A/F at 25°C

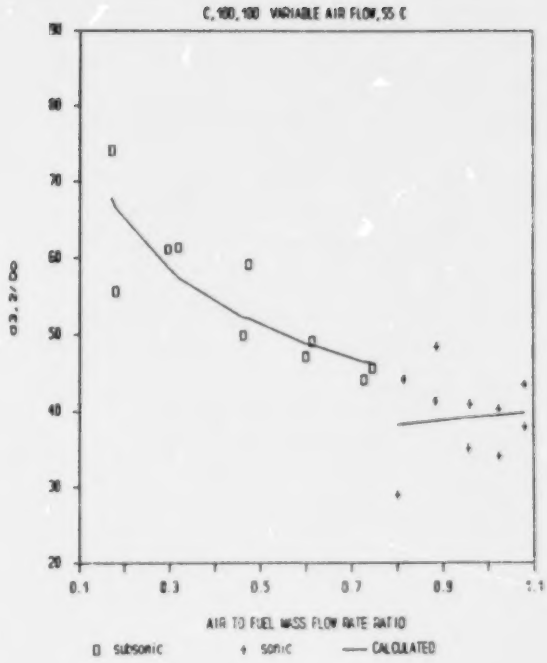

Figure 33 C,100,100, Variable Air Flow Rate d3,2/Do Versus A/F at 55°C

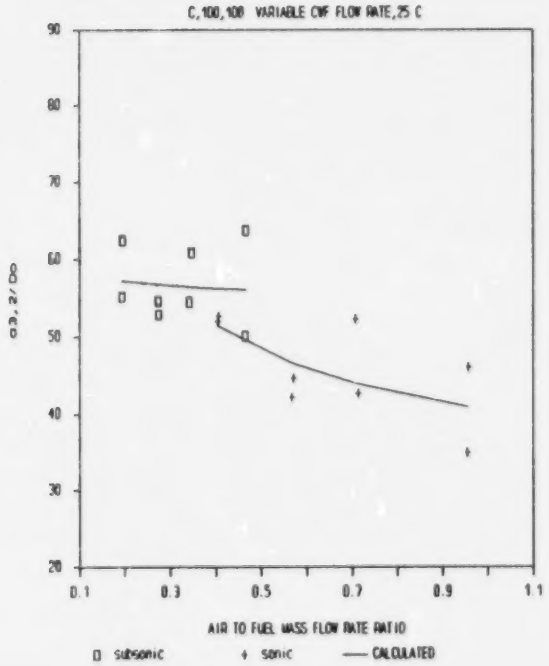

Figure 34 C,100,100, Variable CWF Flow Rate d3,2/Do Versus A/F at 25°C

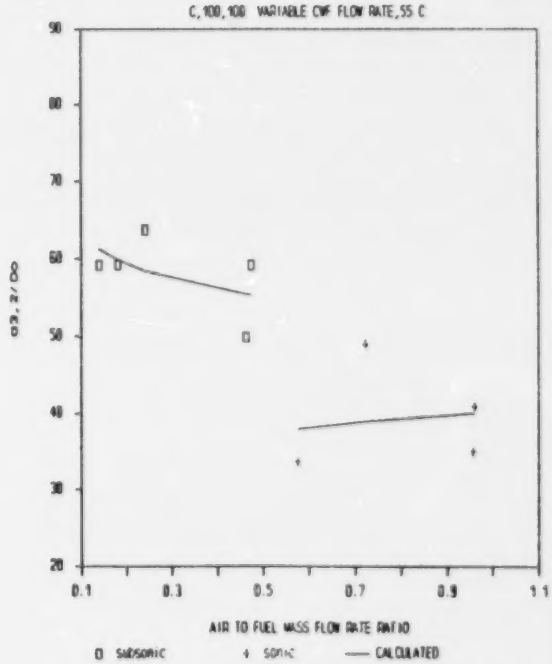

Figure 35 C,100,100, Variable CWF Flow Rate d3,2/Do Versus A/F at 55°C

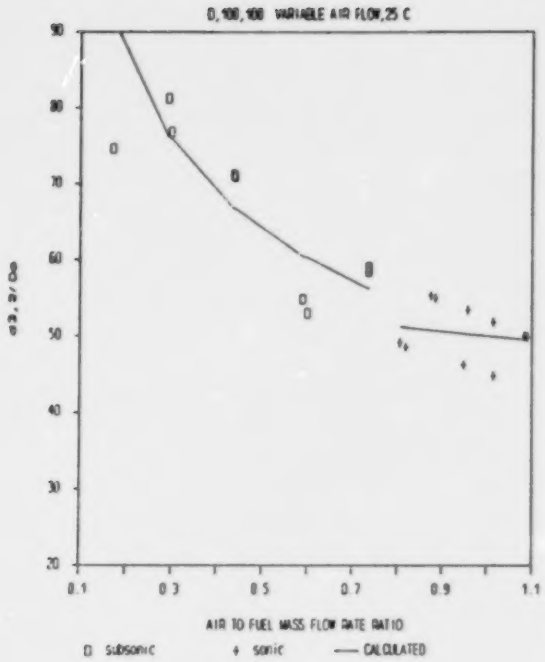

Figure 36 D,100,100, Variable Air Flow Rate d3,2/Do Versus A/F at 25°C

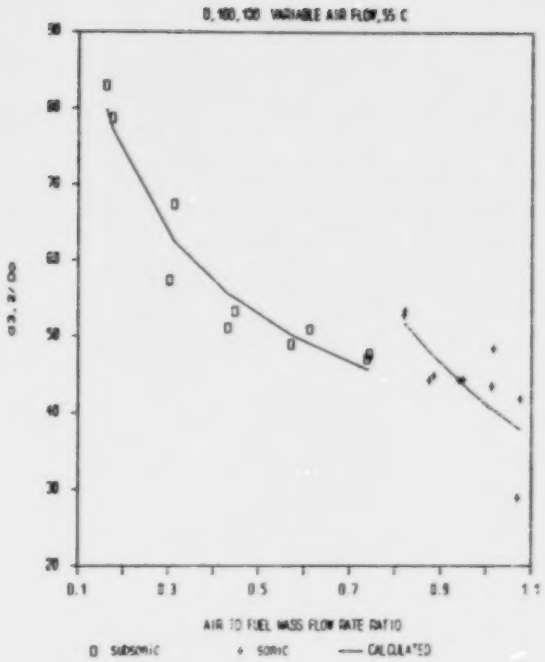

Figure 37 D,100,100, Variable Air Flow Rate d3,2/Do Versus A/F at 55°C

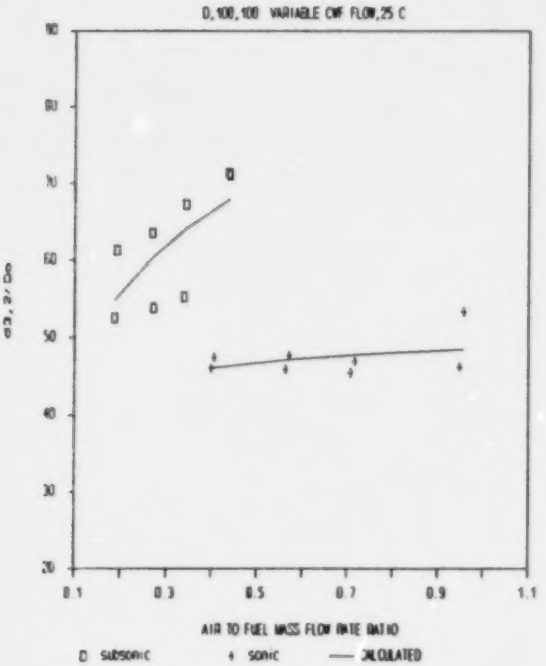

Figure 38 D,100,100, Variable CWF Flow Rate d3,2/Do Versus A/F at 25°C

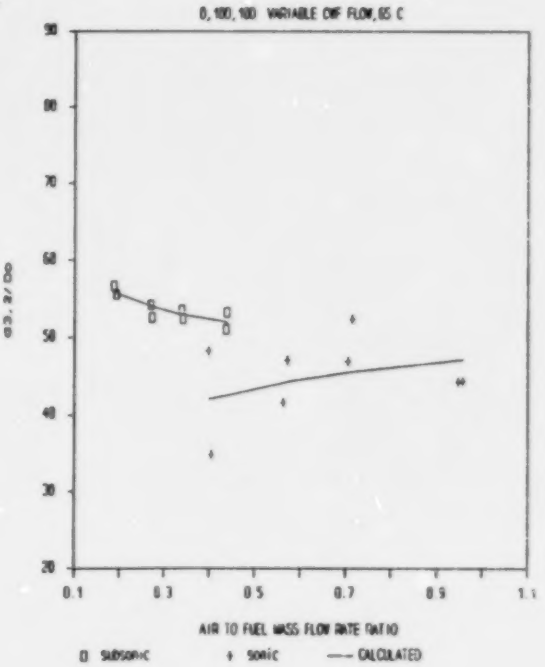

Figure 39 D,100,100, Variable CWF Flow Rate d3,2/Do versus A/F at 65°C

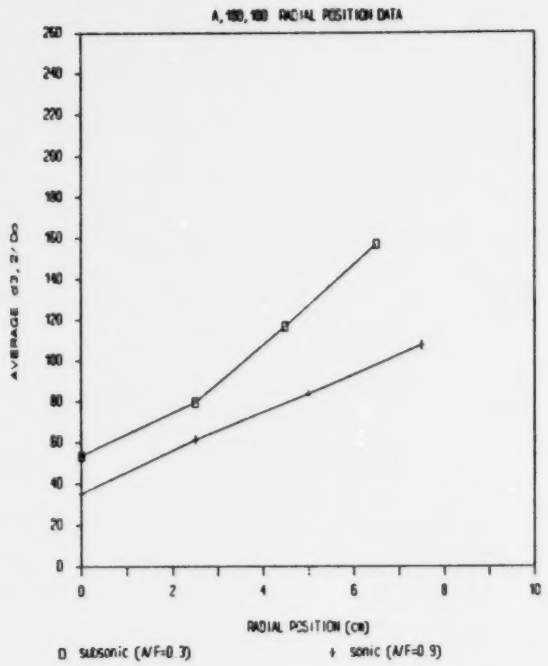

Figure 40 A,100,100, Average d3,2/Do Versus Radial Position

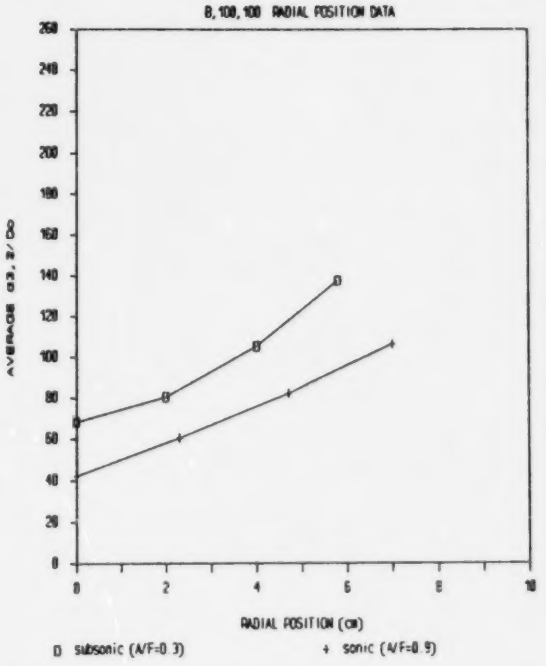

Figure 41 B,100,100, Average d3,2/Do Versus Radial Position

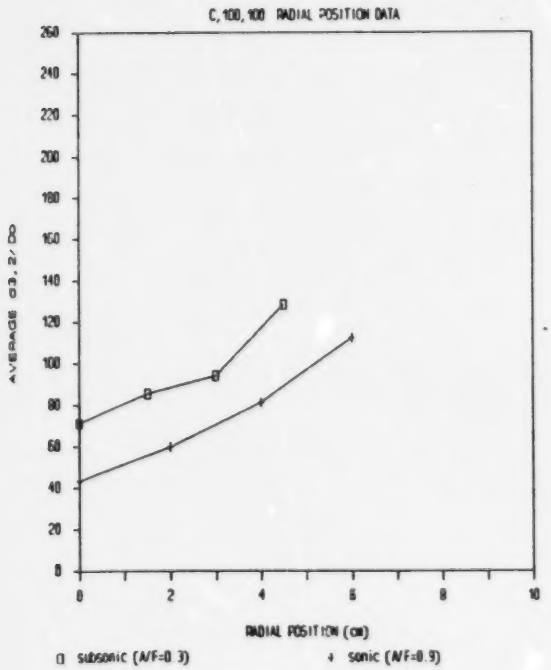

Figure 42 C,100,100, Average d3,2/Do Versus Radial Position

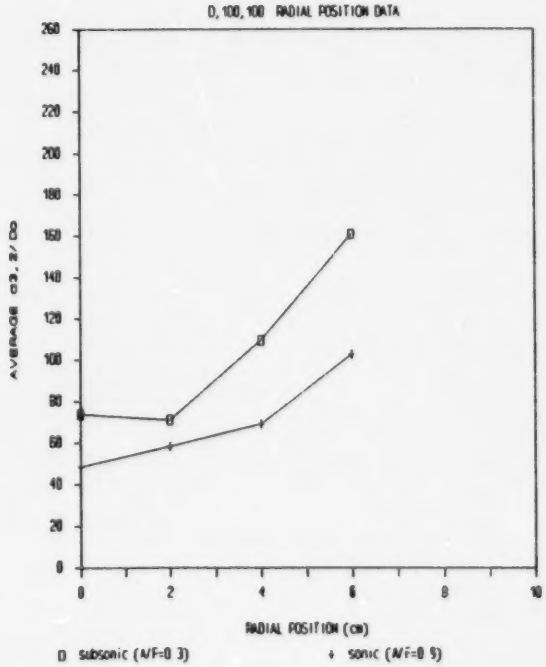

Figure 43 D,100,100, Average d3,2/Do Versus Radial Position

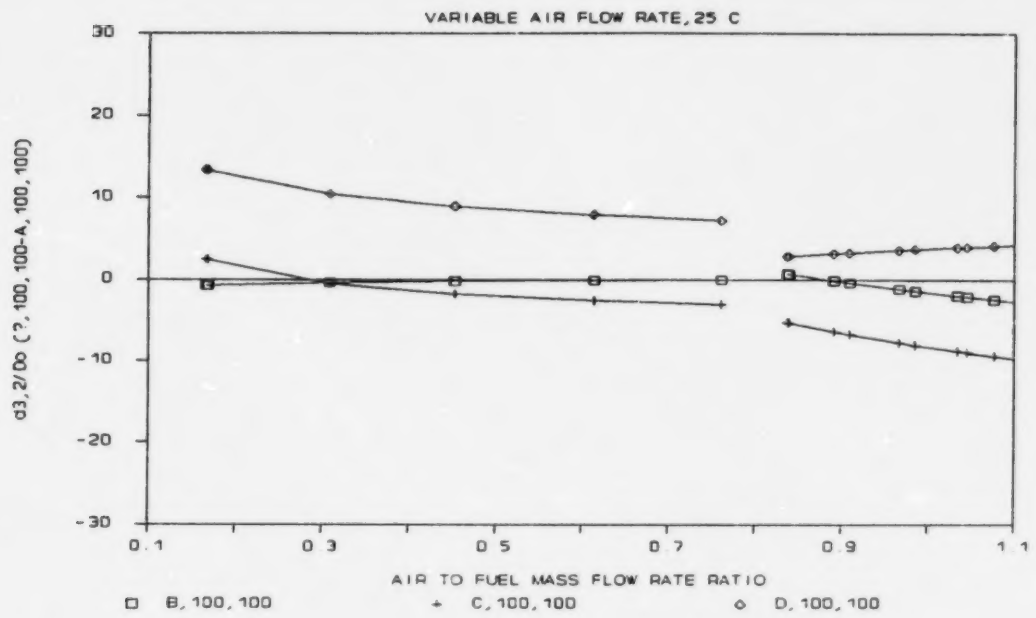

Figure 44 Comparison of d3,2/Do Versus A/F
CWF A, B, C, D, Variable Air Data

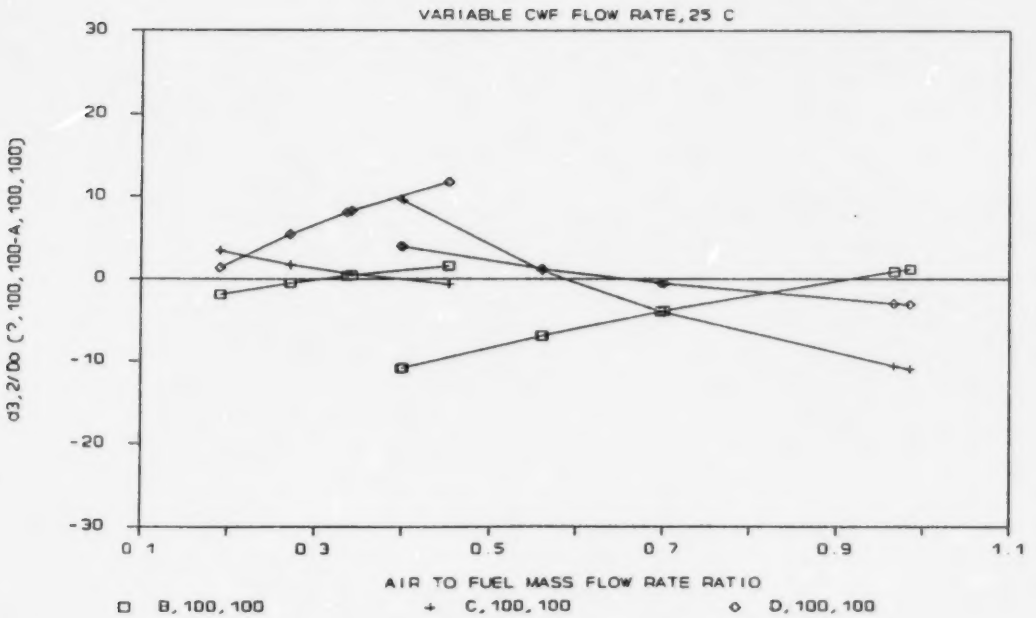

Figure 45 Comparison of d3,2/Do Versus A/F
CWF A, B, C, D, Variable CWF Data

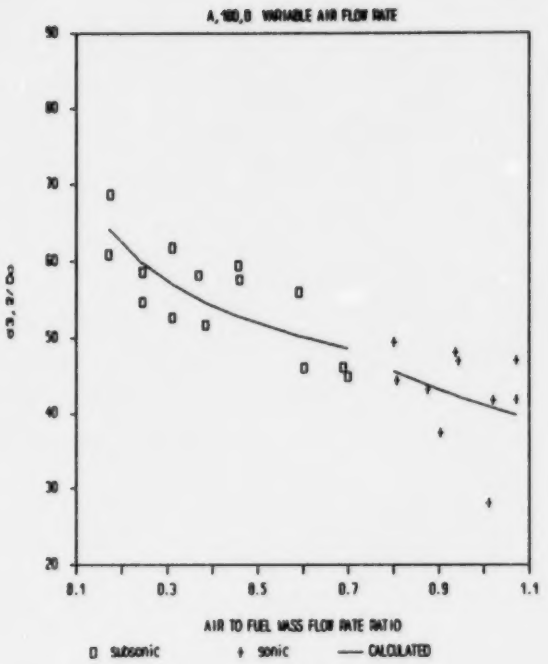

Figure 46 A,100,0, Variable Air Flow Rate d3,2/Do Versus A/F

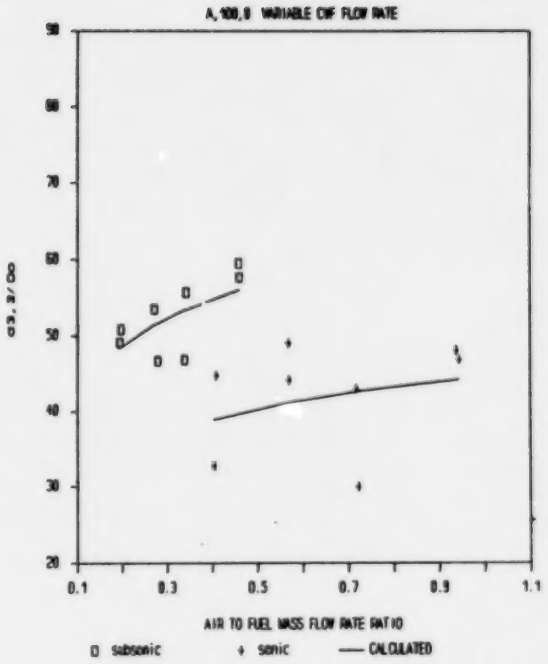

Figure 47 A,100,0, Variable CWF Flow Rate d3,2/Do Versus A/F

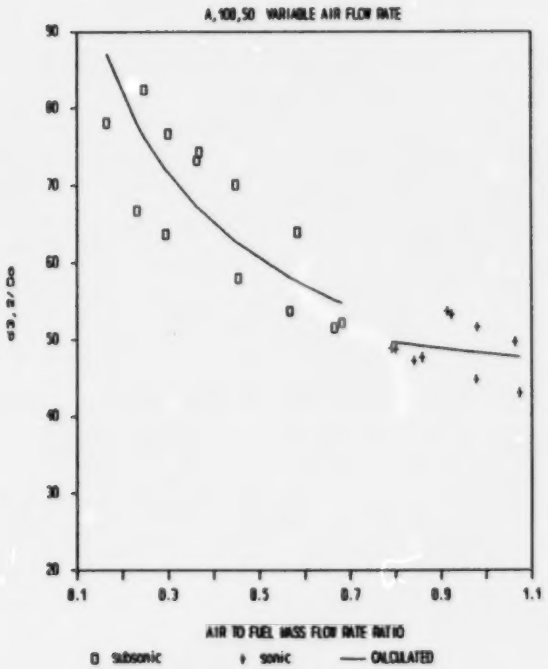

Figure 48 A,100,50, Variable Air Flow Rate d3,2/Do Versus A/F

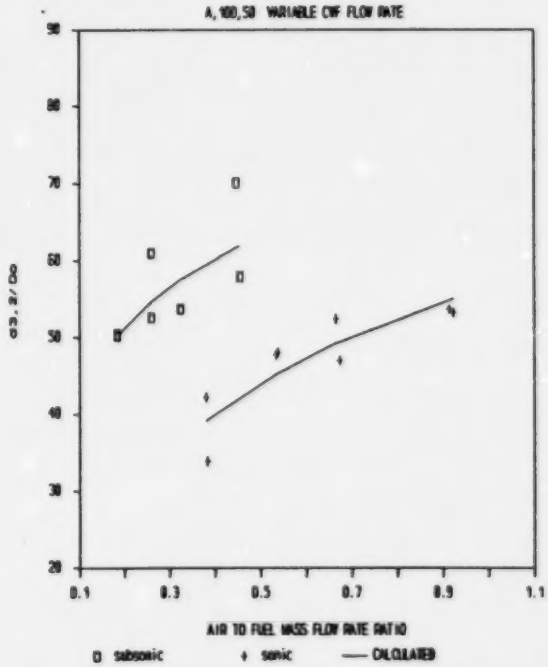

Figure 49 A,100,50, Variable CWF Flow Rate d3,2/Do Versus A/F

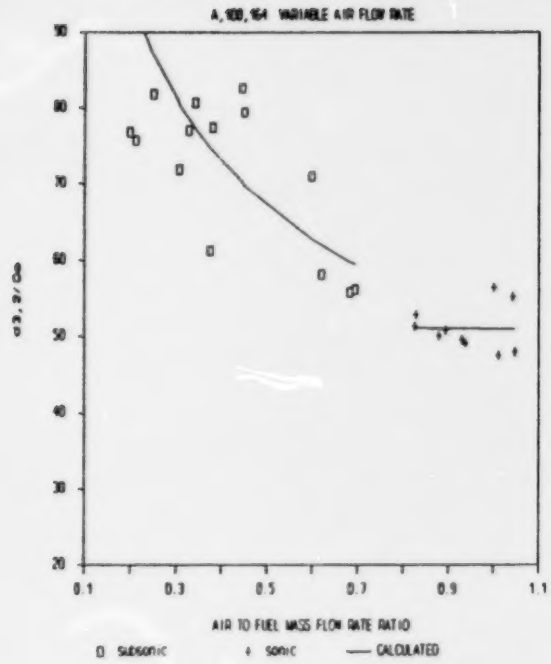

Figure 50 A,100,164, Variable Air Flow Rate d3,2/Do Versus A/F

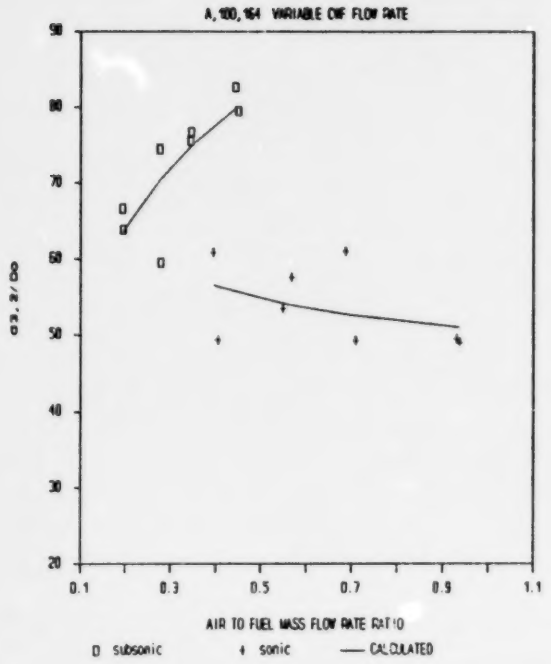

Figure 51 A,100,164, Variable CWF Flow Rate d3,2/Do Versus A/F

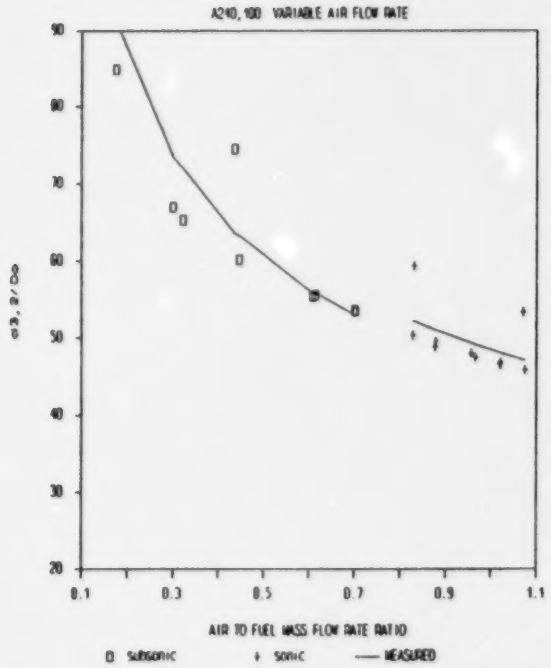

Figure 52 A,240,100, Variable Air Flow Rate d3,2/Do Versus A/F

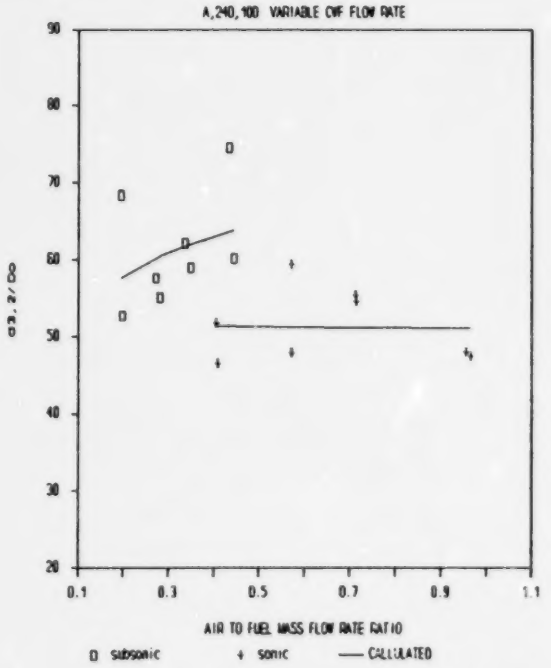

Figure 53 A,240,100, Variable CWF Flow Rate d3,2/Do Versus A/F

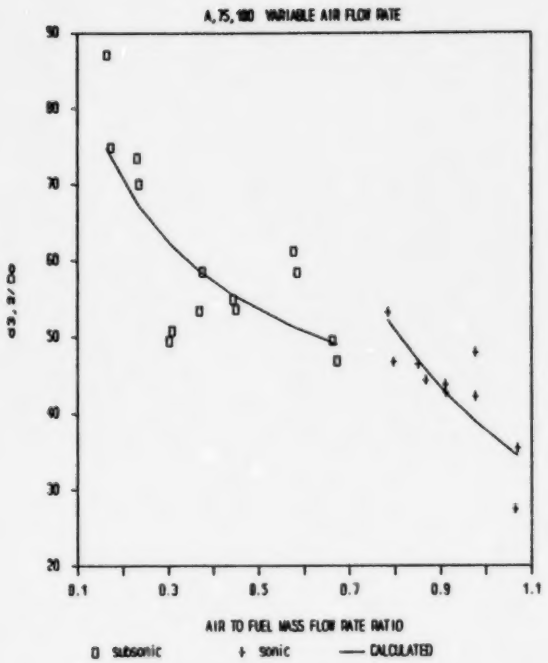

Figure 54 A,75,100, Variable Air Flow Rate d3,2/Do Versus A/F

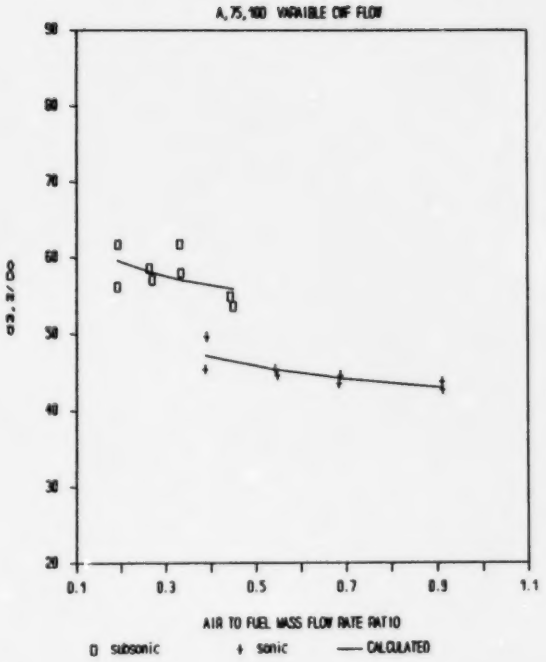

Figure 55 A,75,100, Variable CWF Flow Rate d3,2/Do Versus A/F

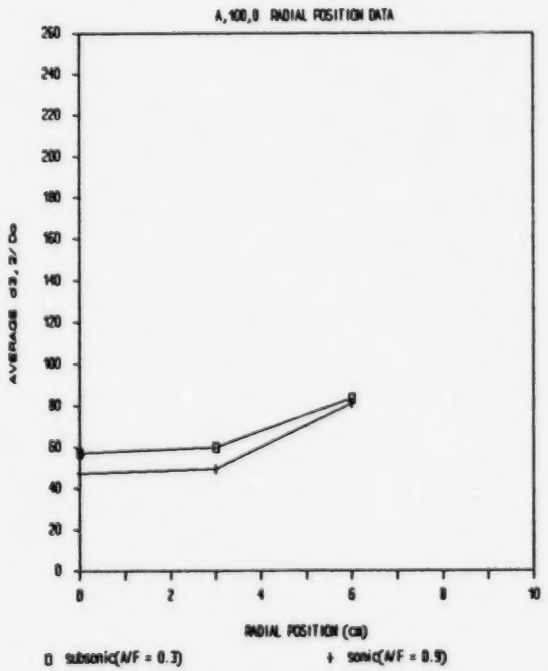

Figure 56 A,100,0, Radial Position Data d3,2/Do Versus A/F

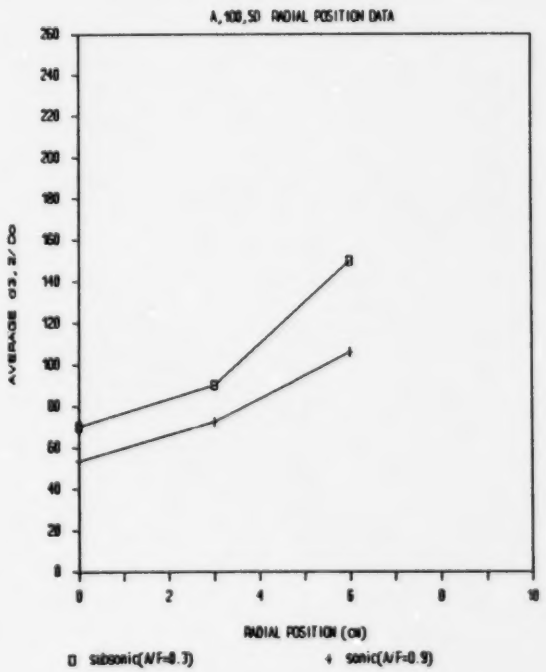

Figure 57 A,100,50, Radial Position Data d3,2/Do Versus A/F

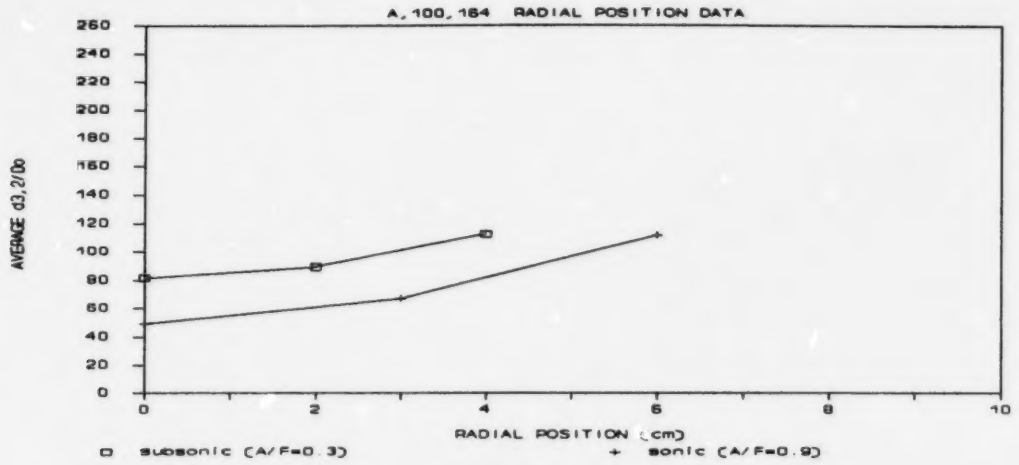

Figure 58 A,100,164, Radial Position Data, d3,2/Do Versus A/F

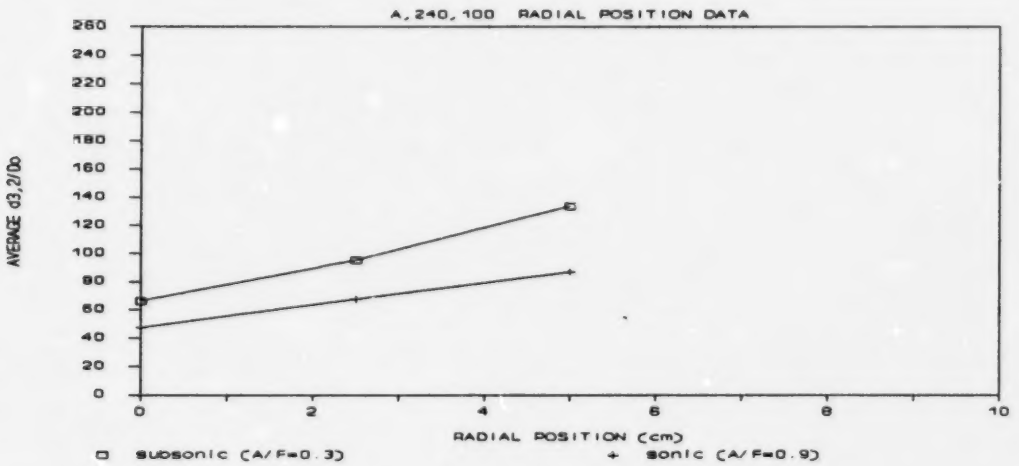

Figure 59 A,240,100, Radial Position Data, d3,2/Do Versus A/F

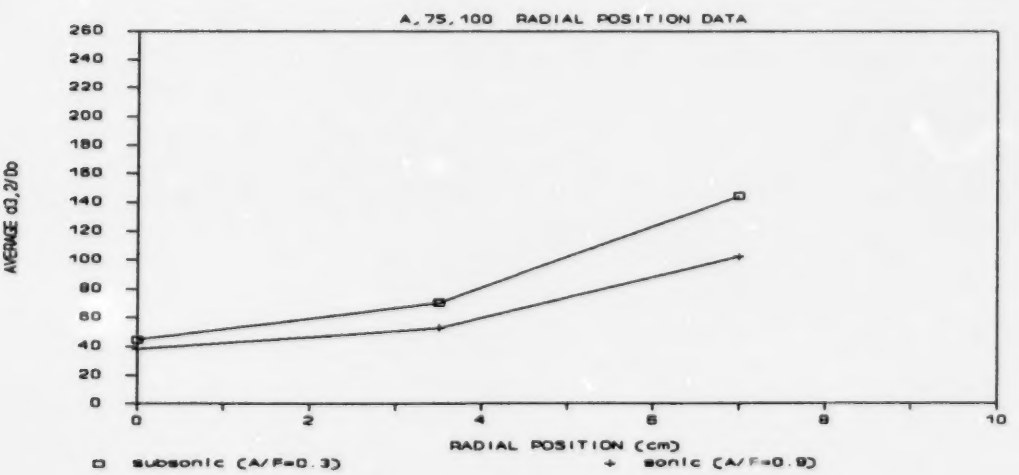

Figure 60 A,75,100, Radial Position Data, d3,2/Do Versus A/F

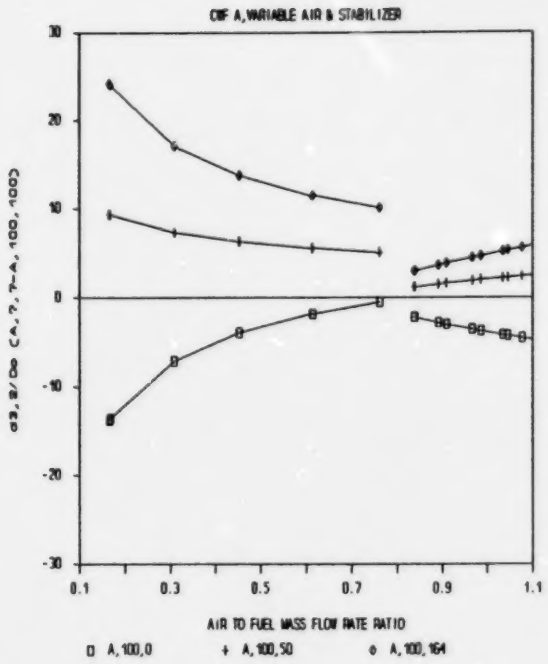

Figure 61 CWF A, Vary Stabilizer
d3,2/Do Versus A/F, Vary Air

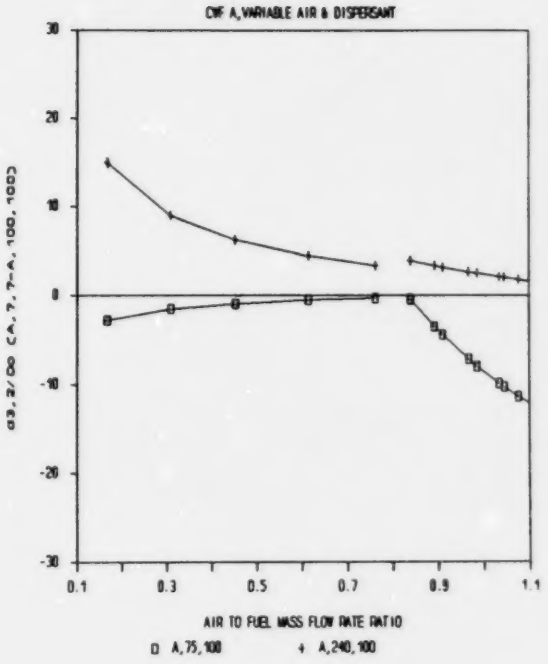

Figure 62 CWF A, Vary Dispersant
d3,2/Do Versus A/F, Vary Air

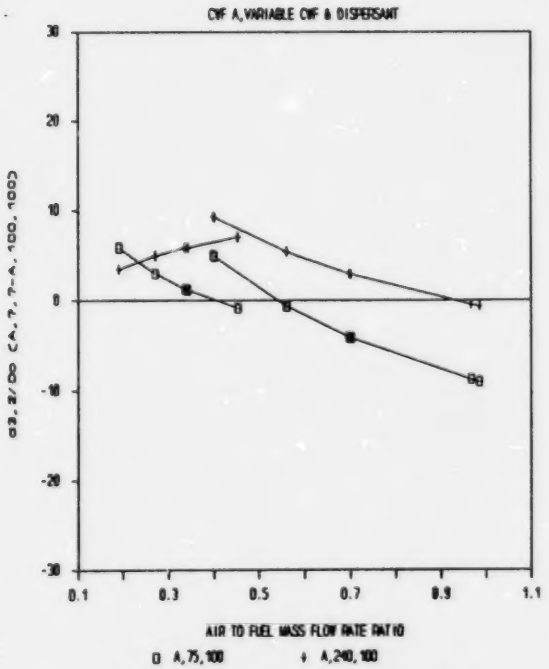

Figure 63 CWF A, Vary Dispersant
d3,2/Do Versus A/F, Vary CWF

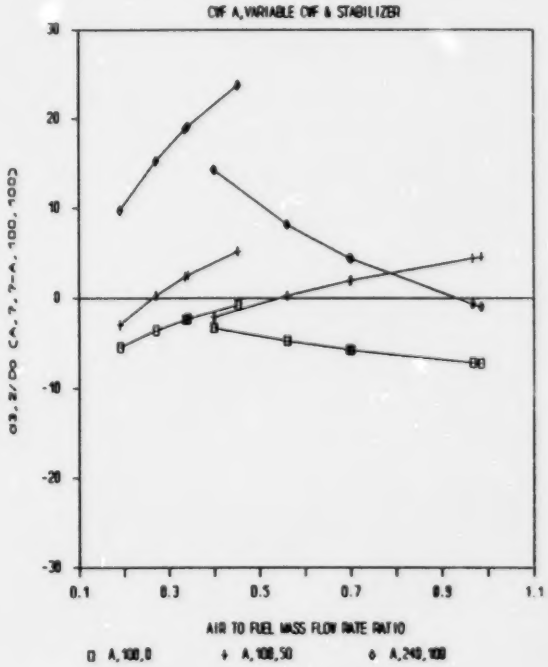

Figure 64 CWF A, Vary Stabilizer
d3,2/Do Versus A/F, Vary CWF

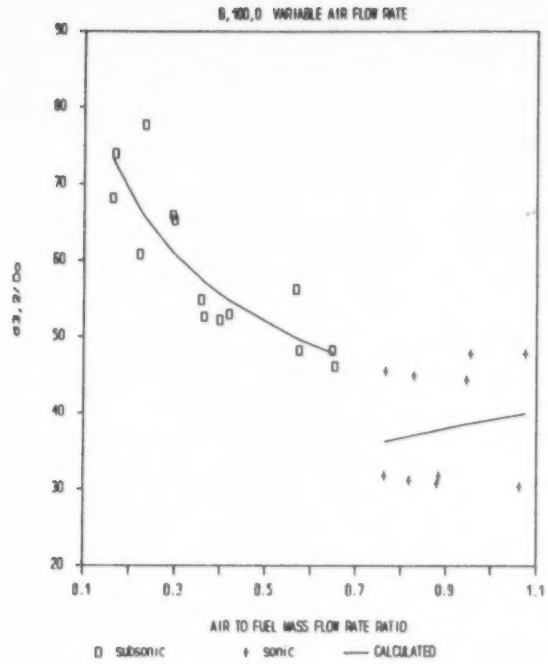

Figure 65 B,100,0, Variable Air Flow Rate d3,2/Do Versus A/F

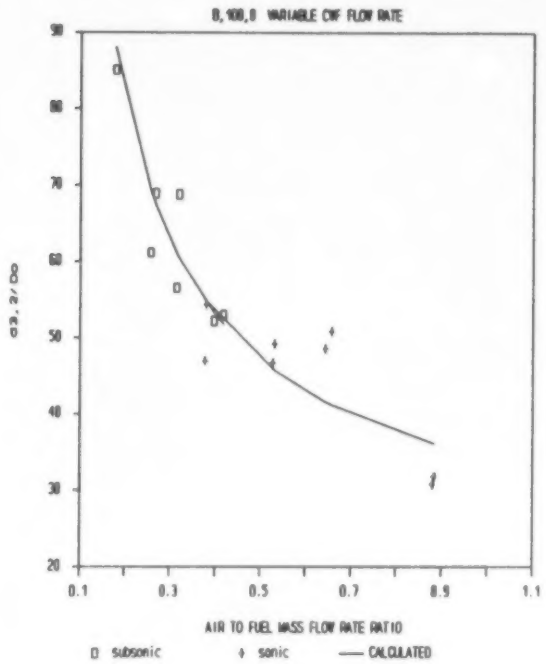

Figure 66 B,100,0, Variable CWF Flow Rate d3,2/Do Versus A/F

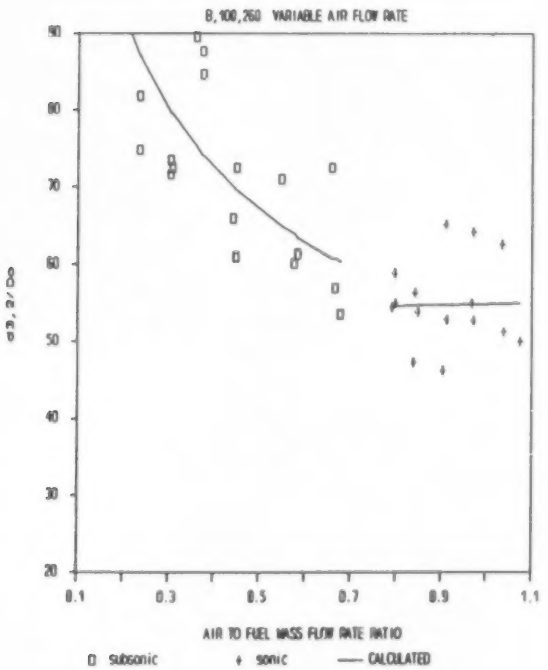

Figure 67 B,100,260, Variable Air Flow Rate d3,2/Do Versus A/F

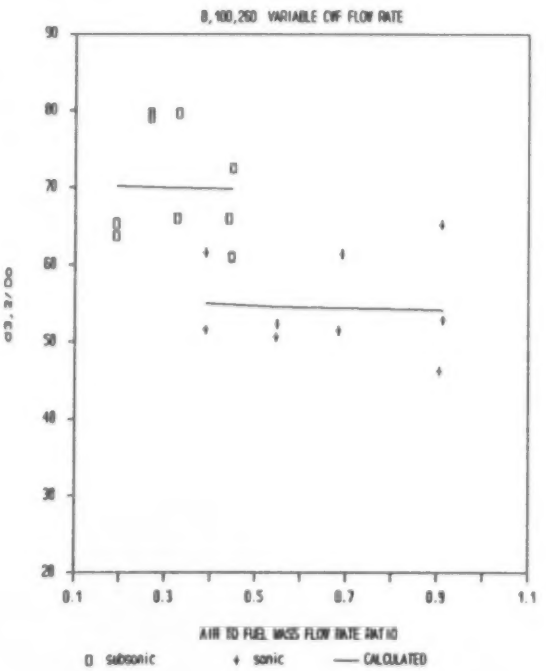

Figure 68 B,100,260, Variable CWF Flow Rate d3,2/Do Versus A/F

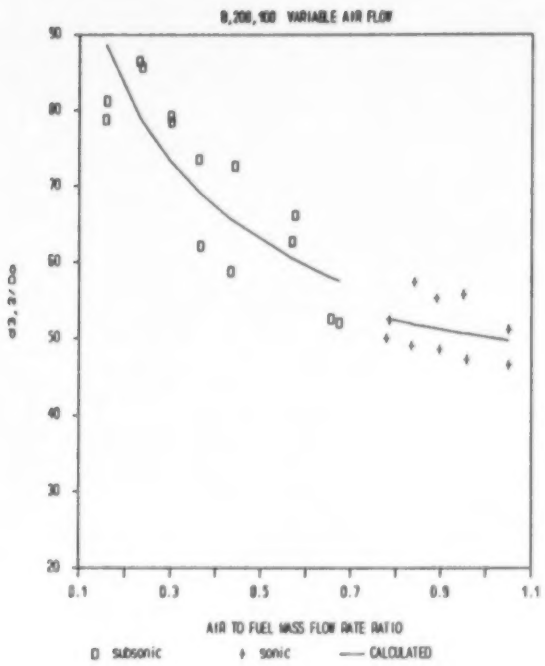

Figure 69 B,200,100, Variable Air Flow Rate d3,2/Do Versus A/F

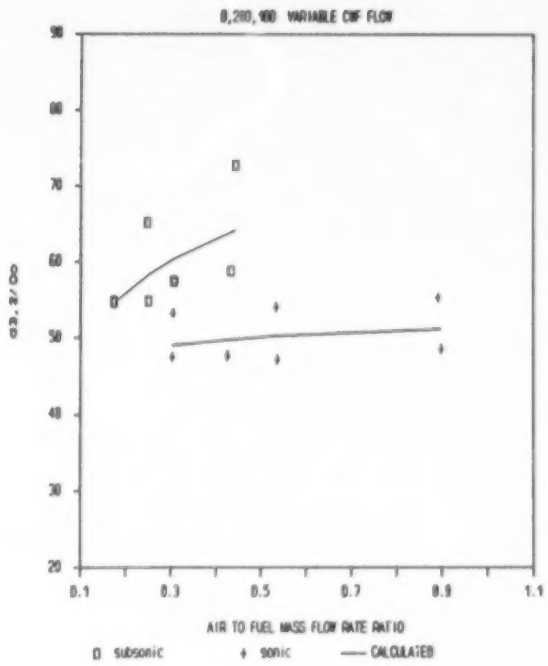

Figure 70 B,200,100, Variable CWF Flow Rate d3,2/Do Versus A/F

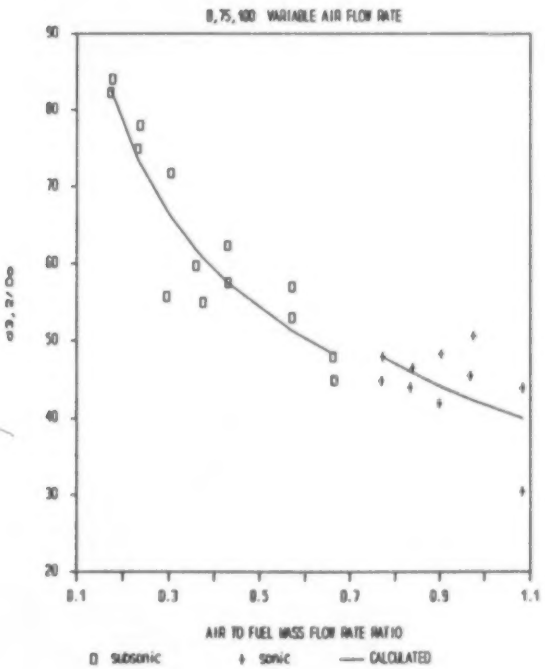

Figure 71 B,75,100, Variable Air Flow Rate d3,2/Do Versus A/F

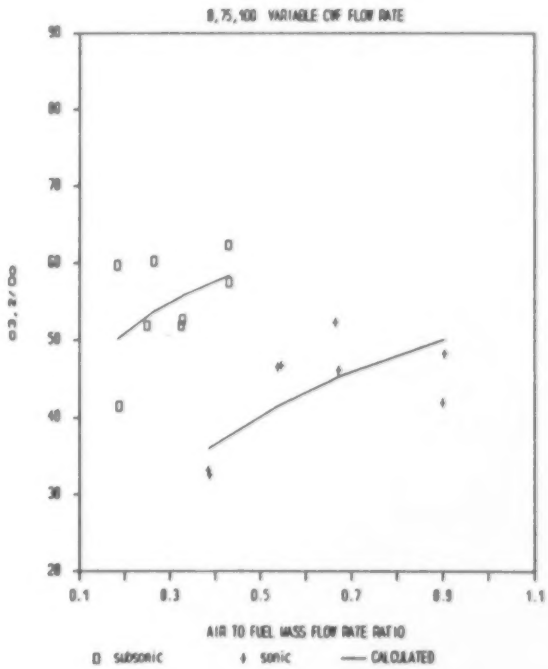

Figure 72 B,75,100, Variable CWF Flow Rate d3,2/Do Versus A/F

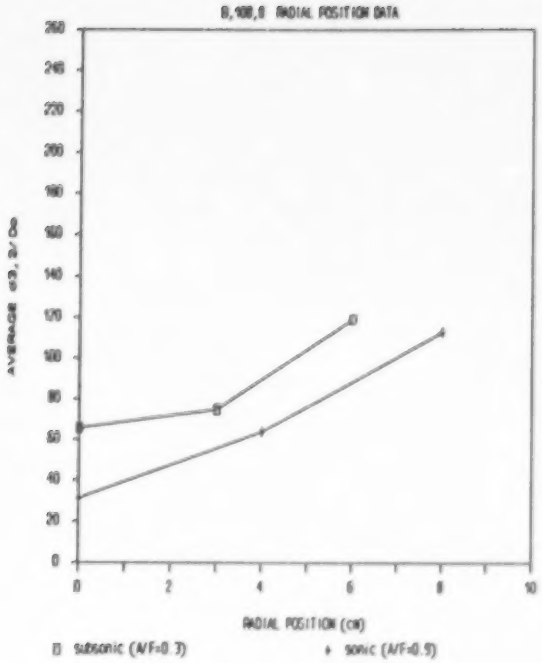

Figure 73 B,100,0, Radial Position Data d3,2/Do Versus A/F

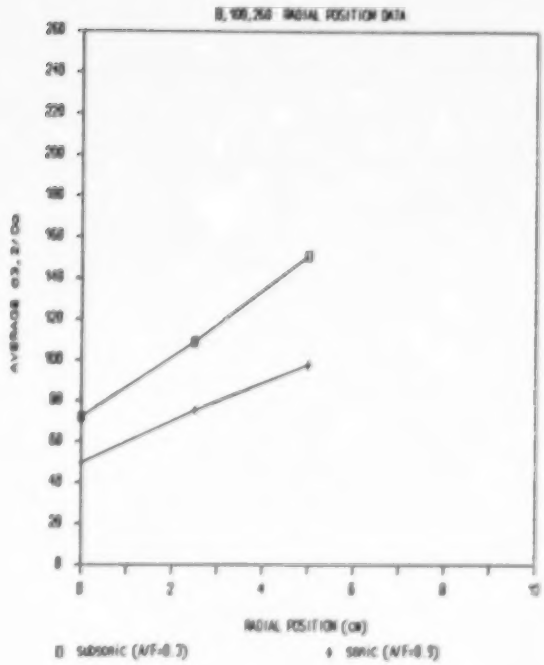

Figure 74 B,100,260, Radial Position Data d3,2/Do Versus A/F

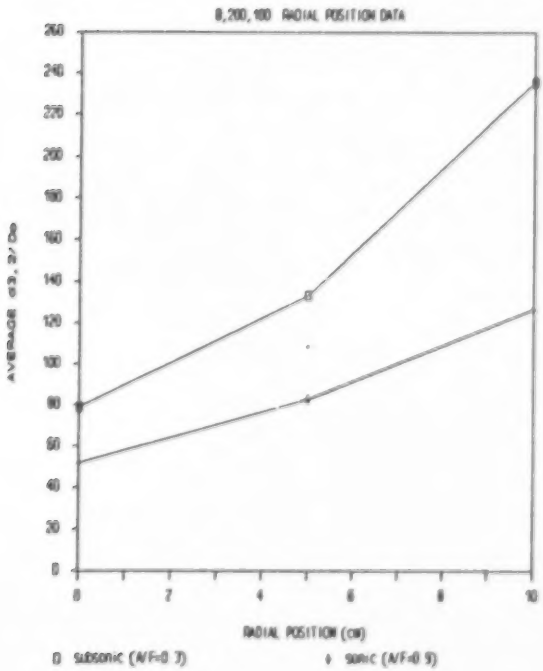

Figure 75 B,200,100, Radial Position Data d3,2/Do Versus A/F

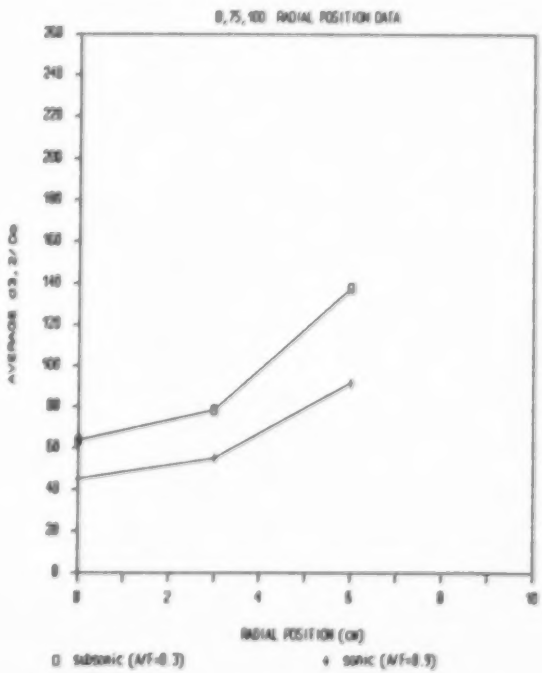

Figure 76 B,75,100, Radial Position Data d3,2/Do Versus A/F

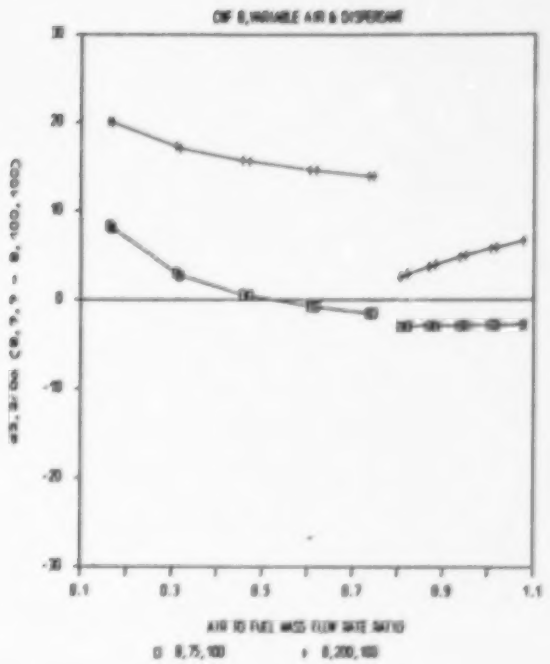

Figure 77 CWF B, Vary Dispersant
d3,2/Do Versus A/F, Vary Air

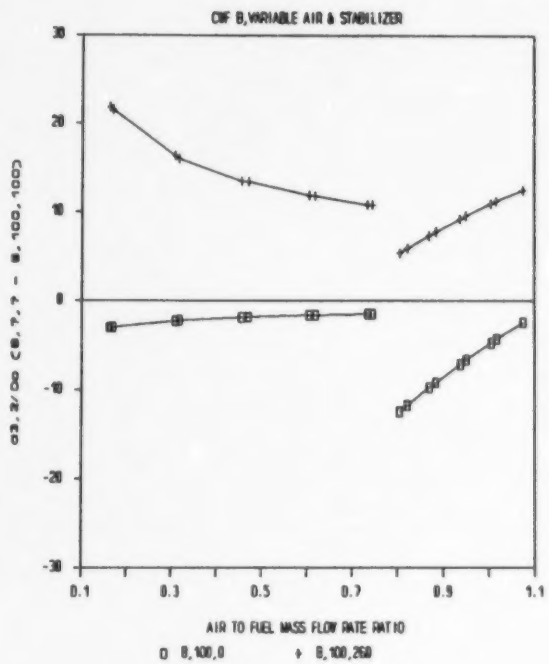

Figure 78 CWF B, Vary Stabilizer
d3,2/Do Versus A/F, Vary Air

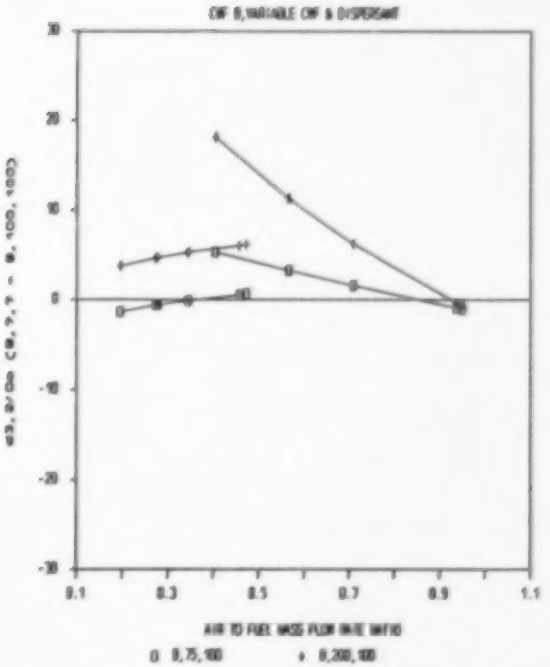

Figure 79 CWF B, Vary Dispersant
d3,2/Do Versus A/F, Vary CWF

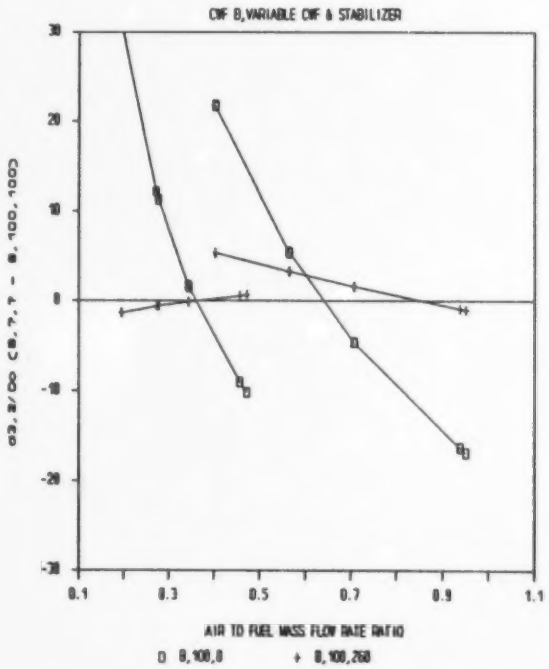

Figure 80 CWF B, Vary Stabilizer
d3,2/Do Versus A/F, Vary CWF

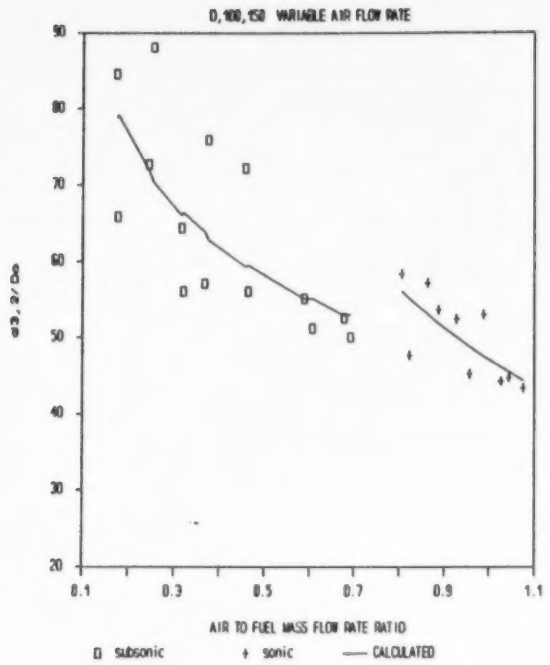

Figure 81 D,100,150, Variable Air Flow Rate d3,2/Do Versus A/F

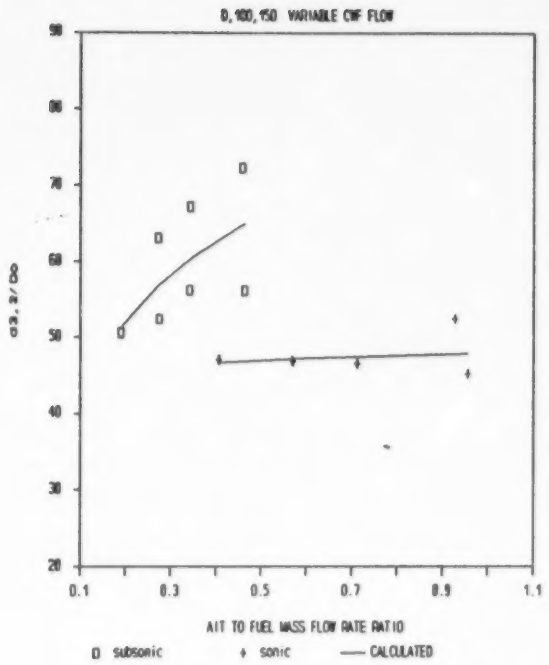

Figure 82 D,100,150, Variable CWF Flow Rate d3,2/Do Versus A/F

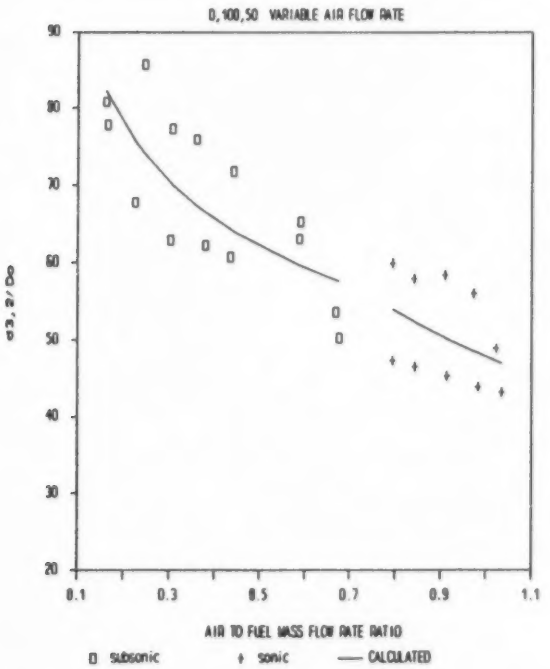

Figure 83 D,100,50, Variable Air Flow Rate d3,2/Do Versus A/F

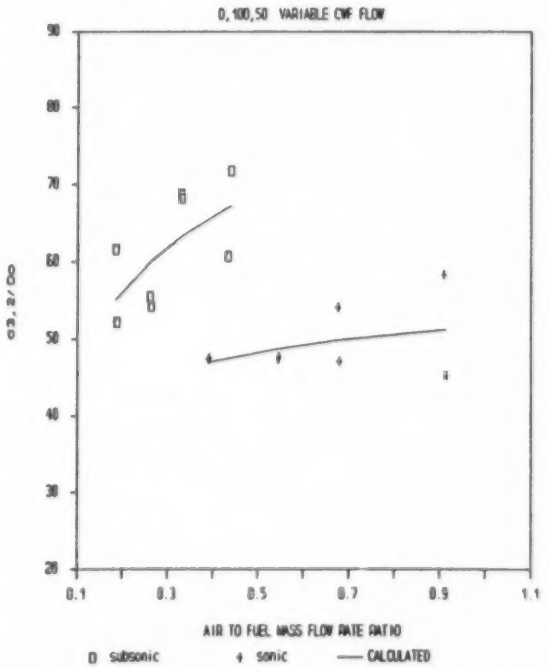

Figure 84 D,100,50, Variable CWF Flow Rate d3,2/Do Versus A/F

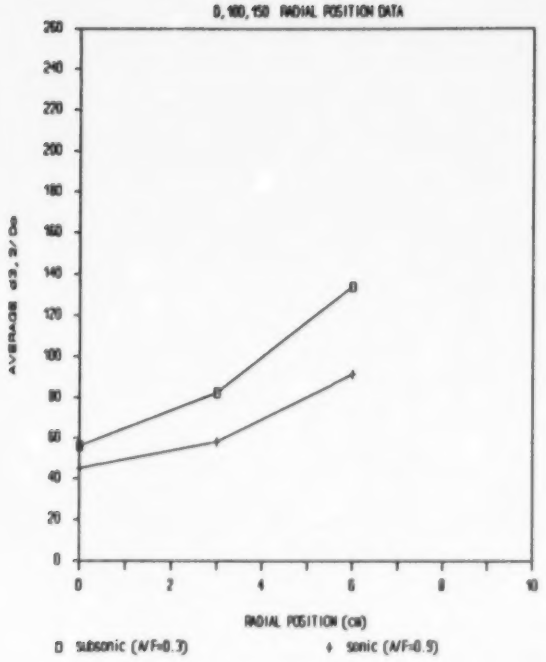

Figure 85 D,100,150, Radial Position Data
d3,2/Do Versus A/F

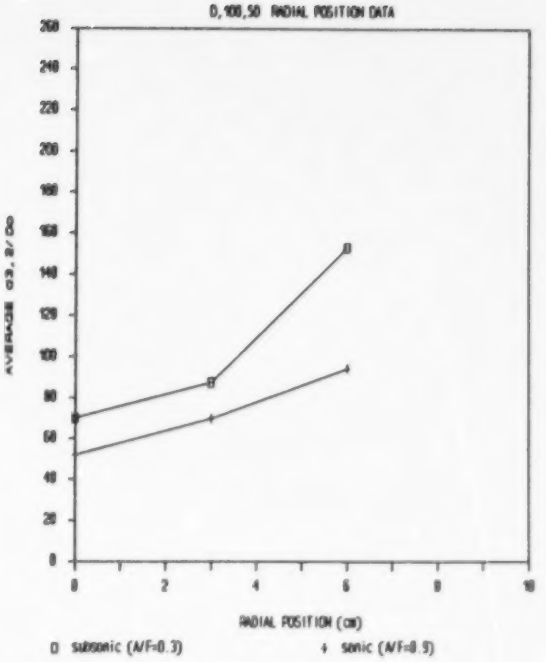

Figure 86 D,100,50, Radial Position Data
d3,2/Do Versus A/F

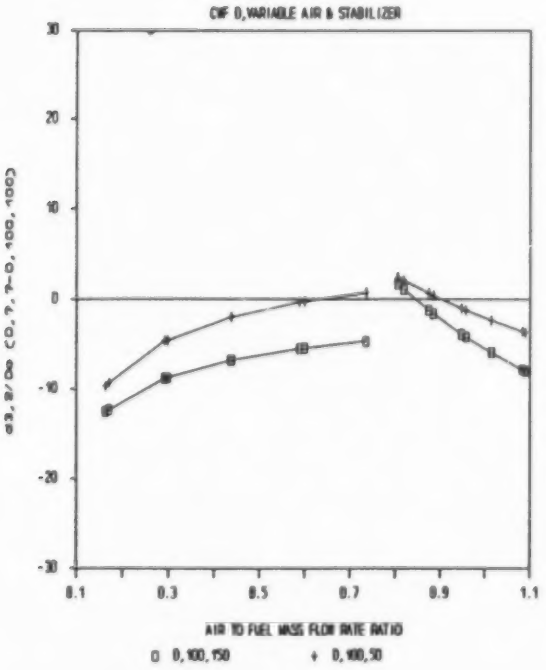

Figure 87 CWF D, Vary Stabilizer
d3,2/Do Versus A/F, Vary Air

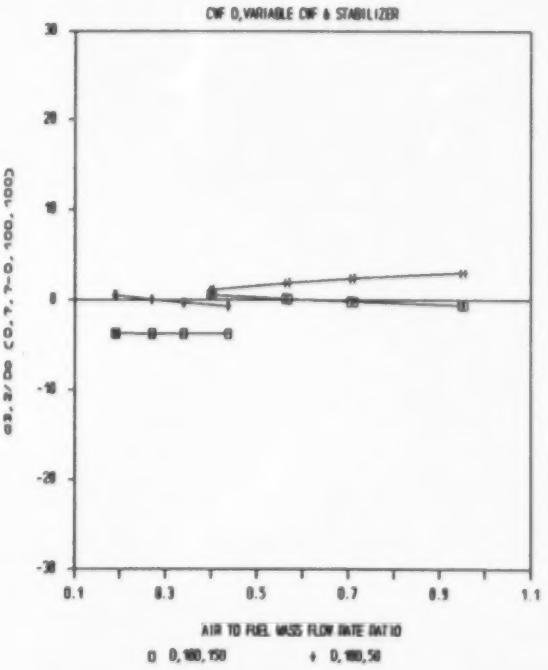

Figure 88 CWF D, Vary Stabilizer
d3,2/Do Versus A/F, Vary CWF

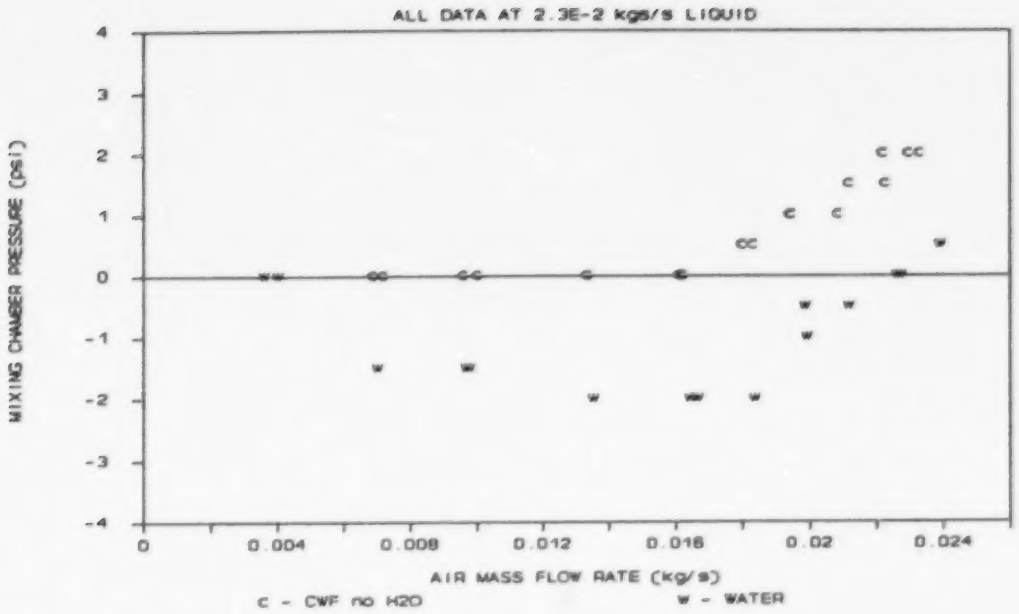

Figure 89 Instrumental Atomizer, Mixing Chamber Pressure Versus Air Mass Flow Rate

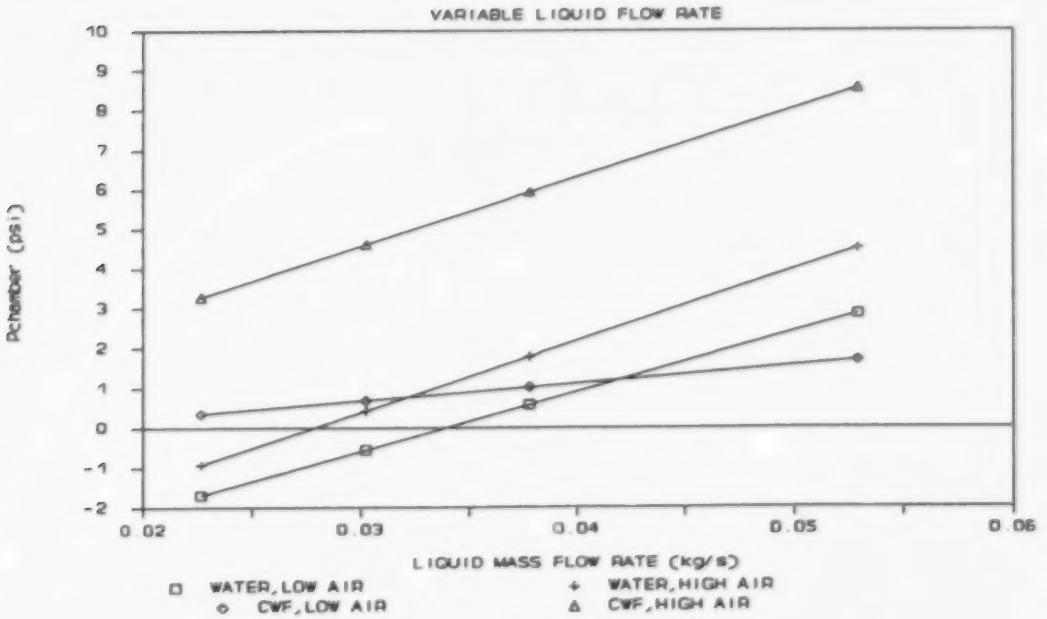

Figure 90 Instrumental Atomizer, Mixing Chamber Pressure Versus Liquid Mass Flow Rate